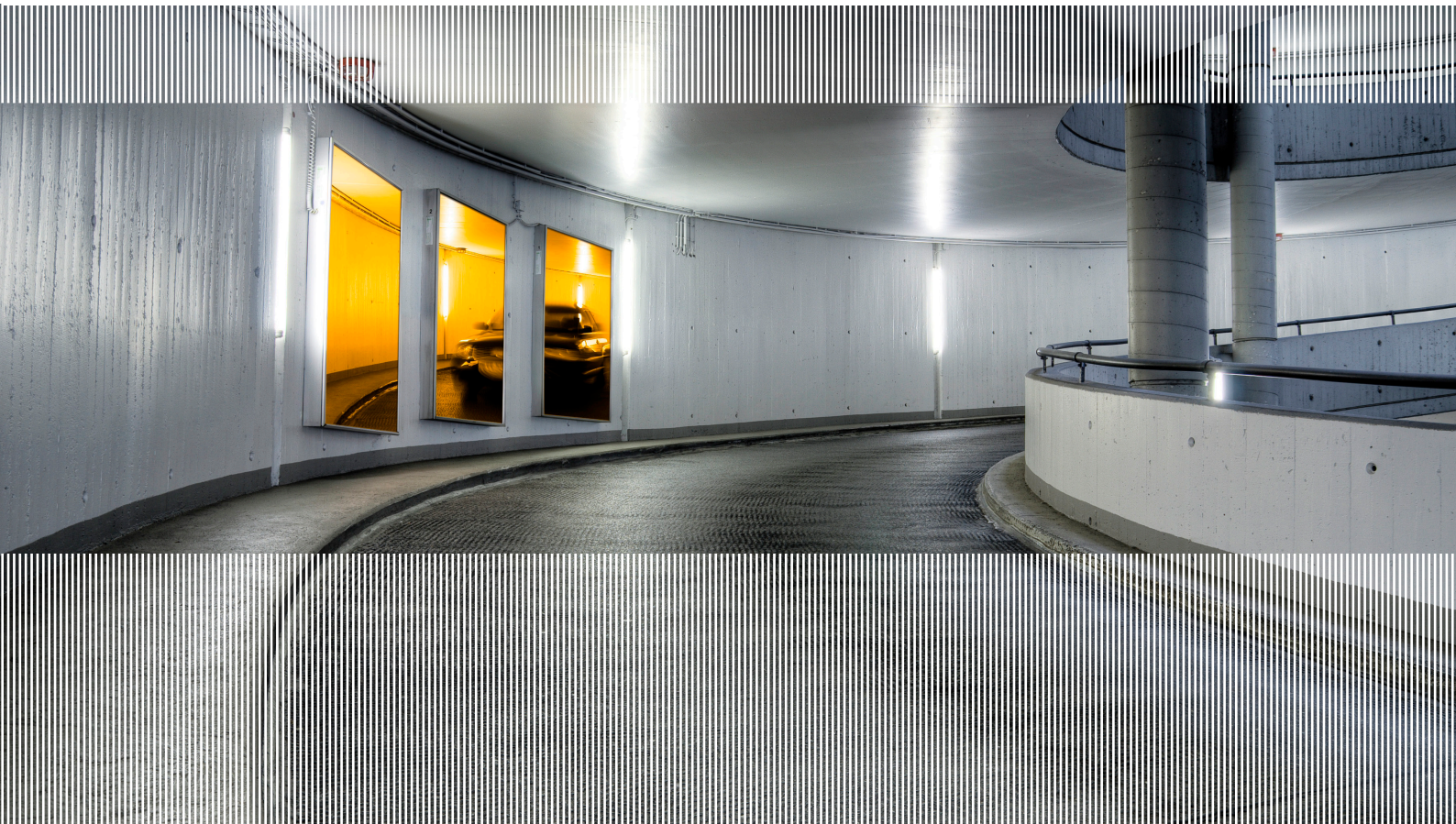


SINTEF Building and Infrastructure Mari Bøhnsdalen Eide and Jorun-Marie Hisdal

Ultra High Performance Fibre Reinforced Concrete (UHPFRC) – State of the art

COIN Project report 44 – 2012



SINTEF Building and Infrastructure

Mari Bøhnsdalen Eide and Jorun-Marie Hisdal

Ultra High Performance Fibre Reinforced Concrete (UHPFRC) – State of the art

FA 2 Competitive constructions

SP 2.2 Ductile high strength concrete

COIN Project report 44 – 2012

COIN Project report no 44

Mari Bøhnsdalen Eide and Jorun-Marie Hisdal

Ultra High Performance Fibre Reinforced Concrete (UHPFRC) – State of the art

FA 2 Competitive constructions

SP 2.2 Ductile high strength concrete

Keywords:

Fiber; Reinforcement; Concrete structures

Project no.: 3D005950

Photo, cover: Garage (iStock)

ISSN 1891–1978 (online)

ISBN 978-82-536-1298-0 (pdf)

ISBN 978-82-536-1299-7 (printed)

38 copies printed by AIT AS e-dit

Content: 100 g Scandia

Cover: 240 g Trucard

© Copyright SINTEF Building and Infrastructure 2012

The material in this publication is covered by the provisions of the Norwegian Copyright Act.

Without any special agreement with SINTEF Building and Infrastructure, any copying and making available of the material is only allowed to the extent that this is permitted by law or allowed through an agreement with Kopinor, the Reproduction Rights Organisation for Norway.

Any use contrary to legislation or an agreement may lead to a liability for damages and confiscation, and may be punished by fines or imprisonment.

Address: Forskningsveien 3 B
POBox 124 Blindern
N-0314 OSLO

Tel: +47 22 96 55 55

Fax: +47 22 69 94 38 and 22 96 55 08

www.sintef.no/byggforsk

www.coinweb.no

Cooperation partners / Consortium Concrete Innovation Centre (COIN)

Aker Solutions

Contact: Jan-Diederik Advocaat

Email: jan-diederik.advocaat@akersolutions.com

Tel: +47 67595050

Saint Gobain Weber

Contact: Geir Norden

Email: geir.norden@saint-gobain.com

Tel: +47 22887700

Norcem AS

Contact: Terje Rønning

Email: terje.ronning@norcem.no

Tel: +47 35572000

NTNU

Contact: Terje Kanstad

Email: terje.kanstad@ntnu.no

Tel: +47 73594700

Mapei AS

Contact: Trond Hagerud

Email: trond.hagerud@mapei.no

Tel: +47 69972000

SINTEF Building and Infrastructure

Contact: Tor Arne Hammer

Email: tor.hammer@sintef.no

Tel: +47 73596856

Skanska Norge AS

Contact: Sverre Smeplass

Email: sverre.smeplass@skanska.no

Tel: +47 40013660

Norwegian Public Roads Administration

Contact: Kjersti K. Dunham

Email: kjersti.kvalheim.dunham@vegvesen.no

Tel: +47 22073940

Unicon AS

Contact: Stein Tosterud

Email: stto@unicon.no

Tel: +47 22309035

Veidekke Entreprenør ASA

Contact: Christine Hauck

Email: christine.hauck@veidekke.no

Tel: +47 21055000

Preface

This study has been carried out within COIN - Concrete Innovation Centre - one of presently 14 Centres for Research based Innovation (CRI), which is an initiative by the Research Council of Norway. The main objective for the CRIs is to enhance the capability of the business sector to innovate by focusing on long-term research based on forging close alliances between research-intensive enterprises and prominent research groups.

The vision of COIN is creation of more attractive concrete buildings and constructions. Attractiveness implies aesthetics, functionality, sustainability, energy efficiency, indoor climate, industrialized construction, improved work environment, and cost efficiency during the whole service life. The primary goal is to fulfil this vision by bringing the development a major leap forward by more fundamental understanding of the mechanisms in order to develop advanced materials, efficient construction techniques and new design concepts combined with more environmentally friendly material production.

The corporate partners are leading multinational companies in the cement and building industry and the aim of COIN is to increase their value creation and strengthen their research activities in Norway. Our over-all ambition is to establish COIN as the display window for concrete innovation in Europe.

About 25 researchers from SINTEF (host), the Norwegian University of Science and Technology - NTNU (research partner) and industry partners, 15 - 20 PhD-students, 5 - 10 MSc-students every year and a number of international guest researchers, work on presently eight projects in three focus areas:

- Environmentally friendly concrete
- Economically competitive construction
- Aesthetic and technical performance

COIN has presently a budget of NOK 200 mill over 8 years (from 2007), and is financed by the Research Council of Norway (approx. 40 %), industrial partners (approx. 45 %) and by SINTEF Building and Infrastructure and NTNU (in all approx. 15 %).

For more information, see www.coinweb.no

Tor Arne Hammer
Centre Manager

Summary

No precise definition of UHPFRC has been found in the reviewed literature, but there seems to be a common understanding that this is a concrete with a compressive strength exceeding 150 MPa. The following characteristics are also prevalent in the literature:

- Direct tensile strength higher than 7-8 MPa
- W/B ratio lower than 0.25, and typically between 0.16 and 0.20
- High content of binder, which leads to the absence of capillary porosity
- Fibres to ensure a ductile behaviour

The difference between UHPFRC and conventional concrete mix design lies in particular in the amount of binder, the size of the aggregate and the presence of fibres. Compared to a conventional concrete, the matrix of the UHPFRC is much denser. In order to produce this type of concrete, it is important to achieve the maximum possible packing density of all granular constituents. Use of a quite large amount of super-plasticizers in order to obtain an acceptable workability is also a characteristic of the UHPFRC.

Sometimes UHPFRCs are subjected to a thermal treatment during curing. The heat treatment initiates the formation of more hydrates, which give the raise to the improved characteristics. The typical compressive strength of UHPC is in the range of 150 – 220 MPa, but higher strengths can be obtained. Still, high compressive strength is not always the most important feature of an UHPFRC; the tensile and flexural strength are often of higher importance.

Without fibres, UHPC can exhibit a direct tensile strength in the range of 7 – 10 MPa. The tensile strength may be doubled when fibres are added to the mix. The increase depends on the amount, type and orientation of the fibres. The flexural strength of UHPFRC is usually much higher than the direct tensile strength. Generally, UHPFRC shows improved characteristics in permeability, heat resistance and impact strength.

Table of contents

PREFACE	3
SUMMARY	4
1 INTRODUCTION	6
1.1 WHAT IS ULTRA-HIGH-PERFORMANCE FIBRE-REINFORCED CONCRETE?	6
1.2 OBJECTIVES	6
2 DEVELOPMENT OF UHPFRC.....	7
2.1 DEVELOPMENT OF UHPFRC	7
2.2 MAIN TYPES OF UHPFRC	7
2.3 SIFCON AND ECC	8
2.4 SUMMARY	9
3 MIX DESIGN.....	11
3.1 GENERAL	11
3.2 MATRIX	11
3.3 AGGREGATES.....	20
3.4 SUPER-PLASTICIZERS	21
3.5 FIBRES	21
3.6 PRODUCTION METHODS	23
3.7 UHPCs WITH COMMONLY AVAILABLE MATERIALS AND/OR TECHNOLOGY	26
3.8 EXAMPLES OF UHPFRCs MIX DESIGN.....	27
4 MATERIAL PROPERTIES.....	29
4.1 MECHANICAL PROPERTIES	29
4.2 PROPERTIES DEPENDENT ON TIME AND/OR TEMPERATURE.....	34
4.3 DURABILITY	35
REFERENCES	37
APPENDIX 1.....	3
AFGC-SETRA, ULTRA-HIGH PERFORMANCE FIBRE-REINFORCED CONCRETE, INTERIM RECOMMENDATIONS: COMPRESSIVE STRENGTH [4].....	3
APPENDIX 2.....	4
AFGC-SETRA, ULTRA-HIGH PERFORMANCE FIBRE-REINFORCED CONCRETE, INTERIM RECOMMENDATIONS: TENSILE BEHAVIOUR [4]	4
APPENDIX 3.....	15
AFGC-SETRA, ULTRA-HIGH PERFORMANCE FIBRE-REINFORCED CONCRETE, INTERIM RECOMMENDATIONS: ANNEX 2 – EXPERIMENTAL PROCEDURE FOR FLEXURAL TENSILE TESTS ON PRISMS AND ANALYSIS METHOD [4]	15

1 Introduction

1.1 What is Ultra-High-Performance Fibre-Reinforced Concrete?

Ultra-high-performance fibre-reinforced concretes are a result of a quest that began in the 1930s. The goal of this quest was to find a way to produce concretes with an improved compressive strength. [1]

No precise definition of UHPFRC has been found in the reviewed literature, but there seems to be a common understanding that this is a concrete with a compressive strength exceeding 150 MPa. It is not sufficient to have an ultra-high compressive strength alone, as these concretes are very brittle - the performance of the concrete must also be ultra-high. The following characteristics are also prevalent in the literature:

- Direct tensile strength higher than 7-8 MPa
- W/B ratio lower than 0.25, and typically between 0.16 and 0.20
- High content of binder, which leads to the absence of capillary porosity
- Fibres to ensure a ductile behaviour

[2-4]

Ultra-High-Performance Fibre-Reinforced Concrete (UHPFRC) is in other words a composite material which differs from an ordinary concrete in many ways. Mechanical properties like compressive and tensile strengths are much higher compared to a conventional concrete. This makes it possible to make slender constructions because now a smaller cross section can transfer the same force as a larger cross section. Due to the very dense matrix UHPFRC has outstanding durability properties. It is shown that the concrete is very resistant to chloride and other chemical attacks and has a high abrasion and fire resistance. The enhanced performance in strength and durability make the concrete suitable for many applications.

1.2 Objectives

This State of The Art Report aims to give an overview on the topic of Ultra-High Performance Fibre-Reinforced Concrete. The topic itself is very large, and this overview seeks to touch the different subtopics essential for UHPFRC without the possibility to treat them all in large detail. This report will focus mainly on the material – mix design and the most relevant mechanical properties – with focus on recent advances.

The report is a part of the work within COIN FA 2.2 High Tensile Strength All-Round Concrete and COIN FA 3.3 Structural Performance, and it will be the basis for further material development within these focus areas. The report is especially relevant for the development of fibre reinforced concrete in general, fibre reinforced lightweight aggregate concrete and a recently established sub-project: ductility of LWAC. Furthermore the report can also serve as basis for new structural concepts proposed within COIN.

2 Development of UHPFRC

2.1 Development of UHPFRC

During the 1930s Eugène Freyssinet demonstrated that pressing concrete during setting could increase its strength, and in the 1960s compressive strengths up to 650 MPa were achieved in small concrete and mortar specimens by simultaneously pressing and heating in a water saturated atmosphere (steam).[1]

The development of what we now characterise as UHPFRC started in the 1970s by Brunauer, Odler and Yudenfreund. They investigated high strength cement pastes with water-cement ratios as low as 0.2-0.3. These low w/c-ratios gave concretes with low porosities leading to compressive strengths up to 200 MPa and low dimensional changes.[5]

The use of super-plasticizers and pozzolanic admixtures is essential in UHPFRC and in the 1980s two new approaches to UHPFRC emerged as a result of the development of the super-plasticisers and pozzolanic admixtures:

- The first approach is called Densified Small Particles (DSP). It is a granular matrix and the compressive strength varies between 150 and 400 MPa. In DSP concrete the used aggregate is extremely hard, like for example calcined bauxite or granite. Further, the concrete has a very high super-plasticizer and silica fume content. This decreases the porosity which increases material strength.
- The second approach is called Macro Defect Free (MDF) concrete. This is a polymer modified cementitious material, where polymerization fills the pores in the concrete leading to extremely strong and compact matrices. However, MDFs have very demanding manufacturing conditions, are water-susceptible and suffer from excessive creep.

[1, 5]

2.2 Main types of UHPFRC

Both MDF and DPS are too brittle for use as a construction material, and adding fibres is required to improve ductility. Because adding fibre to the highly viscous MDF-concrete matrix would cause enormous placing problems, researchers and manufactures have concentrated on adding fibres to DSP matrix. The result is today's UHPFRC[1]. In the last years, the development of UHPFRC has followed three main approaches. Based on these, UHPFRCs are divided into three major types by Pierre Rossi[6]:

Type 1: UHPFRCs with high proportions of short fibres

In 1987 Aalborg Portland (Denmark) developed a concrete with metal fibre content between 5 to 10 % by volume, where the fibre length do not exceed 6 mm. The diameter is 0.15 mm which gives an aspect ratio $l/d \leq 40$. The concrete has been marketed as *Compact Reinforced Composites* (CRC®). This type UHPFRC is used in structures with a high percentage of traditional reinforcement. The short fibres enhance the tensile strength of the concrete, but have little effect on the ductility. A combination with traditional reinforcement is required to prevent brittle failure.

Type 2: UHPFRCs with intermediate proportions of long fibres

Bouygues (France) developed a concrete which has been marketed as *Reactive Powder Concrete* (RPC). Examples of commercialised products based on this concept are DUCTAL® and CERACEM®, which were introduced in the late 1990s. The fibre content for this UHPFRC range between 2 and 3 % by volume, and the length of the fibres are between 13 and 20 mm. Since these fibres enhance both the tensile strength and ductility, the fibres are intended to replace all or part of the reinforcing bars that normally are used in prestressed or reinforced concrete elements.

Type 3: UHPFRCs with a very high proportions of fibres of various lengths

Finally, Laboratoire Central des Ponts et Chaussées (LCPC, France) developed a concrete with a mixture of short and long metal fibres which is known as *Multi Scale Fiber Reinforced Concrete* (MSFRC). An example of this product is CEMTECMultiscale®, which was introduced in France in 2000. The fibre content of this type UHPFRC can be up to 11 % by volume and the fibres can range from shorter than 1 mm and up to 20 mm. The fibres in type 3 concretes increase both the tensile strength and the ductility, and can replace all traditional reinforcing bars in a structural element.

2.3 SIFCON and ECC

Two other types of fibre reinforced concretes are also of interest when talking about UHPFRC, despite the fact that they do not have the ultra-compact matrix with ultra-high strength. The reason they are of interest is they are ductile and show a strain-hardening behaviour, meaning that they undergo multi-cracking under tension.

SIFCON

Slurry-infiltrated-fibered (SIFCON) concrete was presented by Lankard in 1984 as a concept of how one could increase the fibre content to as high as 15-20 % [7]. This results in a very high tensile and flexural strength, impact resistance and crack control. A concrete with such an amount of fibres is not workable, and the technique is developed as to avoid problems with placing. SIFCON is produced by pre-packing the formwork with steel fibres, and then injecting a fine-grained cement-based slurry. This slurry must be very liquid with a w/c-ratio considerably higher than what is normal for fibre-reinforced concretes [1]. Lankard reported compressive strengths between 80 and 200 MPa, and flexural strength up to 75 MPa [7].

Fibres with a high specific surface area must be used, due to the low direct tensile strength of the matrix. The fibre orientation in the placing process can cause the material to be highly anisotropic, and SIFCON therefore has different properties in the different loading directions. A beam can have very high flexural strength, but at the same time perform poorly when it comes to shearing or localised forces. The low strength matrix containing a high percentage of long fibre, leading to multi-cracking of the material, is what results in the very ductile behaviour. [1]

ECC

Engineered cementitious composites (ECC) contain small synthetic fibres with a length of 20 mm and a diameter of 0.05 mm. ECC do not show very high compressive strength (approx.

70 MPa) or tensile strength, but in direct tension these composite materials show strain-hardening behaviour and multi-cracking. They are therefore ductile.[1]

The synthetic fibres have a low density (lower than 1.5) and high elastic modulus (higher than 40 GPa). Because of the low density and a high surface area of the fibres, a maximum of 2% can be added before leading to workability problems. The very high length-diameter ratio of the fibres make fresh ECC very viscous, and is therefore not easily placed using conventional techniques.[1]

2.4 Summary

In March 2012 the 3rd International Symposium on Ultra-High Performance Concrete and Nanotechnology for High Performance Construction Materials was held in Kassel, Germany. In their conference article [8], Naaman and Wille sums of both the Advances in matrix and fibres since the 1960's (Figure 1) and the developments in high-strength high-performance cement composites from the 1970's in the USA and Europe (Figure 2).

Decade	Cementitious Matrix and Concrete	Fiber
1970's	<ul style="list-style-type: none"> Better understanding of hydration reactions; gel structure; Better understanding shrinkage, creep, porosity, ... High strength concrete to 50 MPa in practice Development of water reducers Advances in concrete treatments and curing conditions 	<ul style="list-style-type: none"> Smooth steel fibers; normal strength Glass fibers Some synthetic fibers
1980's	<ul style="list-style-type: none"> Increased development of chemical additives: HWRA, etc... Increased utilization of fly ash and silica fume, and other mineral additives, etc... Increased flowability (flowable concrete) Reduction in W/C ratio; High-Strength-Concrete terminology: up to 60 MPa; special high strength: up to 80 MPa; exotic high strength (special aggregate and curing): up to 120 MPa High-Performance-Concrete terminology: high-strength-concrete with improved durability properties. 	<ul style="list-style-type: none"> Deformed steel fibers: normal and high strength Low-modulus synthetic fibers (PP, nylon, etc..) Increased use of glass fibers Micro fibers High performance polymer fibers (carbon, Spectra, Kevlar, etc..)
1990's	<ul style="list-style-type: none"> Increased development in chemical additives: superplasticizers; viscosity agents; etc.... Increased use of supplementary cementitious materials as cement replacement UHPC: application of concept of high packing density; addition of fine particles; low porosity; lower water to cementitious ratio; Self consolidating concrete; self compacting concrete; 	<ul style="list-style-type: none"> New steel fibers with a twist (untwist during pull-out) PVA fibers with chemical bond to concrete Improved availability of synthetic fibers
2000's	<ul style="list-style-type: none"> Increased developments of proprietary and non-proprietary UHPC/UHP-FRC UHPC: improved understanding of high packing density; application of nanotechnology concepts 	<ul style="list-style-type: none"> Ultra high strength steel fibers: smooth or deformed with diameters as low as 0.12 mm and strengths up to 3400 MPa Carbon nano-tubes; carbon nano-fibers
2010's	<ul style="list-style-type: none"> Increased understanding of the cementitious matrix at the nano-scale ...??? 	<ul style="list-style-type: none"> Carbon nano-fibers, graphene,???

Figure 1 Chronological Advances in the matrix and fibres since the 1960's [8]

Year	f_c (MPa)	Source/Ref.	Name	Special Conditions
1972	230	Yudenfreund, Skalny, et al.		Paste; vacuum mixing; low porosity; small specimens.
1972	510	Roy et al. (US)		Paste; high pressure and high heat; small specimens.
1981	200	Birchall et al. (UK)	MDF (Micro-Defect-Free)	Paste; addition of polymer; bending strength up to 150 MPa
1981-1983	120 to 250	Bache; Hjorth (Denmark)	DENSIT; COMPRESSIT	Mortar and concrete; normal curing; use of microsilica
1980's all	120 to 250	Bache; Young; Jennings; Aitcin (Denmark; US; Canada)	DSP (Densified Small Particles)	Improved particle packing; use of microsilica; use of superplasticizers;
1980's	Up to 120	Many researchers worldwide (Shah; Zia; Russell; Swamy; Malier; Konig; Aitcin; Malhotra)	High Strength Concrete; High Performance Concrete (HSC; HPC)	Concrete with special additives and aggregates for structural applications; use of superplasticizers; normal curing; better durability
1980's all	Up to 210	Lankard; Naaman (US)	SIFCON (Slurry Infiltrated Fiber Concrete)	Fine sand mortar with high volume fractions of steel fibers (8% to 15% by volume)
1987	Up to 140	Bache (Denmark)	CR (Compact Reinforced Concrete)	Concrete with high volume of steel fibers used with reinforcing bars
1987	Open range	Naaman (US)	HPFRCC (High Performance Fiber Reinforced Cement Composites)	Mortar and concrete with fibers leading to strain-hardening response in tension
1991	Open range	Reinhardt and Naaman (Germany, US)	HPFRCC (First International Workshop)	Toward reducing the fiber content.
1992	Open range	Li and Wu (US)	ECC (Engineered Cementitious Composites)	Mostly mortar with synthetic fibers; strain-hardening behavior in tension
1994	In excess of 150	De Larrard (France)	Ultra-High Performance Concrete (UHPC)	Optimized material with dense particle packing and ultra fine particles
1995	Up to 800	Richard & Cheyrezy	RPC (Reactive Powder Concrete)	Paste and concrete; heat and pressure curing; particle packing
1998 and later	Up to 200	Lafarge; (Chanvilliard; Rigaud; Behloul) France	DUCTAL	90°C heat curing for 3 days; steel fibers up to 6% (commercially available)
2000 and later	Up to 200	Rossi et al. LCPC (France)	CEMTEC; CEMTEC-multi-scale	Up to 9% fibers; hybrid combinations
Early 2000	Up to 200	Many researchers worldwide (Ulm, Graybeal, Rossi)	UHPC and UHP-FRC	Many formulations based on DUCTAL
2005	Up to 140	Karihaloo (UK)	CARDIFRC	Optimized particle packing and mixing procedure
2005	Up to 200	Jungwirth (Switzerland)	CERACEM	Formulation similar to DUCTAL, larger fibers, larger aggregates
2004	Open range >150	Fehling & Schmidt (Germany)	First International Symposium on UHPC	Many formulations similar to DUCTAL with and without heat curing; with and without fibers.
2005	Open	Schmidt et al. (Germany)	Sustainable Building with UHPC	German DFG funded broader initiative (2005-2012)
2008	Open range >150	Fehling & Schmidt (Germany)	Second International Symposium on UHPC	Many formulations similar to DUCTAL with and without heat curing; with and without fibers.
2011	>150	Accorsi & Meyer (US)	UHPC Workshop	First US Workshop
2011	Up to 290	Wille & Naaman (US-Germany)	UHP-FRC	No heat curing; optimized packing; record direct tensile strength
2011			ACI UHPC Committee 239	First meeting: Oct. 2011 Also: PCI working group
2012	Open range >150	Fehling & Schmidt (Germany)	Third International Symposium on UHPC	

Figure 2 Developments in high-strength high-performance cement composites from the 1970's to date (in the US and Europe) [8]

3 Mix design

3.1 General

UHPFRC is composed of aggregates, cement, water, additives, admixtures and fibres. The difference between UHPFRC and conventional concretes mix design lies in particular in the amount of binder, the size of the aggregate and the presence of fibres. Use of quite a large amount of super-plasticizers in order to obtain an acceptable workability is also a characteristic of the UHPFRC. Compared to a conventional concrete, the matrix of the UHPFRC is much denser. In order to produce this concrete, it is important to achieve the maximum possible packing density of all granular constituents [9]. This gives both improved mechanical and durability properties. The dense matrix is achieved by optimizing the packing density of all granular raw material, i.e. cement, ultra-thin addition (typically silica fume) and aggregate [2].

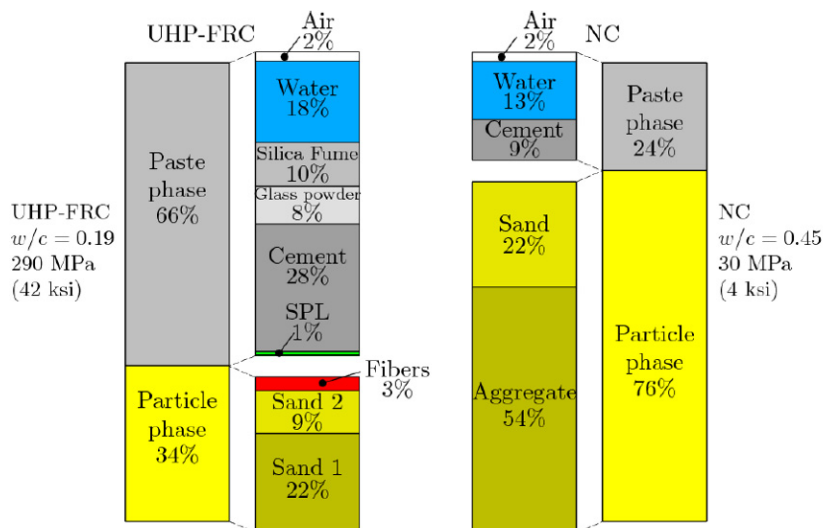


Figure 3 Example of mix proportions by volume comparing UHPFRC with normal concrete [8]

3.2 Matrix

The matrix phase in concrete is defined to consist of free water, additives and all solid particles smaller than 0,125 mm. This includes cement, pozzolanic materials and the filler fraction of the aggregates[10]. The matrix consist therefore of both chemically reactive and inert materials[11]. Some materials function as both chemically reactive and packing density enhancing materials.

Particle packing

Many different materials benefit from densely packed systems, and particle packing is fundamental for concrete. A more densely packed concrete system requires less binder. The main challenge concerning packing and concrete is that the concrete also must obtain an acceptable flow and compatibility in the fresh state. This can be solved by introducing large amounts of fine particles with the same size as cement or below.[7]

The packing density is one of the most important properties of a particle system, and is defined as the volume percentage of solids for each volume unit. If there are smaller sized particles present to fill the voids between the larger sized particles in a system, the packing density will increase. Thus, if we increase the number of size classes available in the system, the achievable packing density increases. Considering the fact that fresh concrete to a certain degree has to flow during placing, a completely dense packing is not suitable. [7] The use of water-reducing agents can help flowing in densely packed systems.

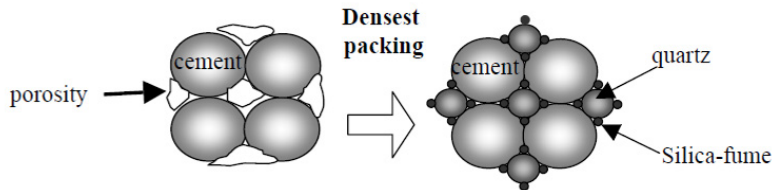


Figure 4 - Packing mix design [12]

The reason we want to achieve a dense particle packing in concrete, is related to what we call the interfacial transition zone (ITZ) around the aggregates. The ITZ is a porous and weak layer of cement paste, which has an increased amount of ettringite and large portlandite (CH) crystals present. The cement particles cannot be packed sufficiently around the aggregates, which results in a layer of cement particles with lower packing density and the presence of micro-bleeding. The more porous structure of the ITZ reduces the tensile and compressive strengths of the concrete. The porous structure also allows enhanced water transport through the ITZ, and deteriorating processes such as alkali-silica reaction, sulphate attack and ingress of chlorides can be increased.[7]

The thickness of the ITZ is influenced by five factors according to Lagerblad and Kjellsen [13]:

1. Packing of particles at the interface
2. Stability of the paste
3. Volume stability of the concrete
4. Cement composition and grinding
5. Chemical reactions at the aggregate surfaces

Adding fillers to the packing system may therefore influence the particle packing and stability of the paste in a positive manner. This is especially true for filler finer than cement.[7]

In addition, a more densely packed system will affect the bond strength between matrix and fibres in fibre-reinforced concrete considerably. More contacts points between matrix and fibre, caused by the finer particles present, will enhance friction during fibre pull-out tests. [14]

In Norway Elkem has been involved in the development of UHPFRC for decades, and has developed a particle packing programme called EMMA (Elkem Materials Mix Analyser).[15]

Water/binder-ratio

The term binder refers to the chemically reactive materials in the matrix, meaning cement and ultra-thin addition, such as silica fume and other pozzolanic materials. A crucial parameter to ensure optimal properties of the mix is the water to binder (w/b) ratio. A w/b-ratio below 0.25 ensures a reasonable balance between the flow properties of the concrete and the strength of the hardened concrete. The w/b ratio for an UHPFRC typically lies between 0.16 and 0.2. [2, 16] In Figure 5 the compressive strength as a function of w/b ratio is given for some typical concretes. As the figure shows, an UHPFRC has a considerable lower w/b ratio than a conventional concrete, for which w/b lies between 0.4 and 0.7.

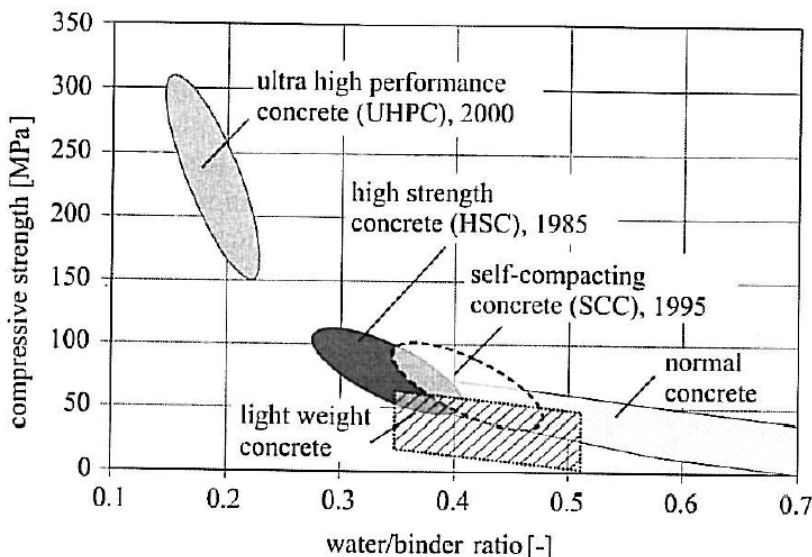


Figure 5 Strength as a function of w/b ratios for different types of concrete [16]

Cement

UHPFRCs make use of approximately twice the amount of cement as a conventional concrete. The cement content normally lies between 600 to 1000 kg/m³. The fineness of the cement should be between 3000 and 4500 cm²/kg. Regarding type of cement, Portland cements with a low C₃A content can be recommended because of their low water demand. This is preferable due to the fact that UHPFRC has a very low water/ binder ratio. Further, this is also advantageous regarding the risk of secondary ettringite formation in case of curing at high temperatures [16]. Due to low water/binder-ratios, not all of the cement particles can react. The remaining cement will act inertly and contribute to the particle packing.

Silica fume

SF is a by-product of the smelting process used to produce silicon metal and ferrosilicon alloys containing more than 75 % silicon. SF generally has the following main characteristics [11] :

- SiO₂ content 85-98 %,

- spherical shape with a mean particle size in the range 0.1 to 0.2 μm and
- an amorphous structure

SF is an essential part of UHPFRC and this principally due to the followings:

- SF reacts with calcium hydroxide (CH), which is a reaction product of the Portland cement hydration, and produces more of the CSH binder. When CH is replaced by CSH, which has a much higher strength, the porosity decreases in the bulk and in particular in the ITZ, which results in a significant increase in strength. [11]
- In order to produce UHPFRC, it is important to achieve the maximum possible packing density of all granular constituents [16].

For a high strength concrete, in particular, it is very useful to regard SF as a water replacement in terms of workability and water demand: In a pure cement paste binder, a certain amount of water is necessary to fill the void space and make flow possible. Addition of water-reducing agents disperses the cement flocks and lowers the void space volume and hence the water demand. Even further water reduction is possible with SF, since it can replace the water in the void space and, at the same time, increase the workability when super-plasticisers are used. It is possible that there exists a “ball-bearing effect “ of the spherical SF-particles that improves the mobility of the irregular cement particles[11].

SF consists of particles which are far smaller than the cement particles (about 1/100). The small size makes SF a very efficient filler [11] and following increases the packing density [16]. To fill the voids between the cement particles, a large quantity of silica fume, amounting about 10-30 % of the cement mass, is required [16]. For comparison a normal structural concrete SF amounts up to 10 % of the total binder contents. [11]

Fly ash

Fly ash (FA) for use in concrete is a by-product from furnaces fired with pulverised coal, often power-plants. The fly ash can be either an aluminosilicate or a calcium silicate, and because of the reactive silicon dioxide (SiO_2) both types contain, fly ash has pozzolanic properties. [17]



Figure 6: Fly ash [18]

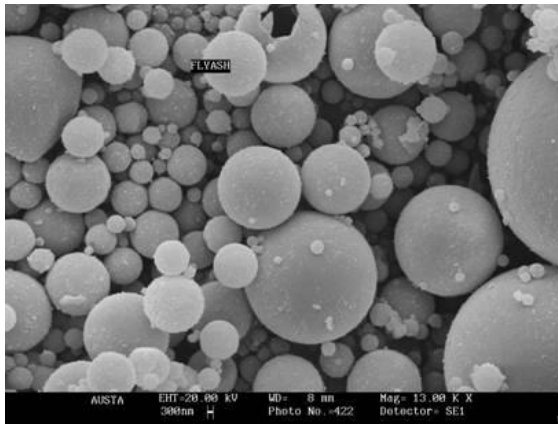


Figure 7 SEM image of fly ash particles[19]

An overview over FAs effects on concrete properties is given by Malhotra and Mehta in [20]:

- Replacing cement with FA will increase setting time and decrease hardening rates in early ages. In a longer perspective, mechanical properties can be improved compared to concretes with only ordinary Portland cement.
- The majority of FA particles have a spherical shape, with a "ball-bearing-effect" enhancing flowability of fresh concrete. FA therefore has a water-reducing effect.
- Concretes with FA has shown a decreased permeability, lower alkali-silica-reaction and reduced sulphate attacks.

Ground Granulated Blast-furnace Slag

Ground Granulated Blast-furnace Slag (GGBS) is made from molten iron slag from a blast furnace, a by-product from the iron and steel industry. The slag is composed of lime, silica and alumina, with small amounts of alkali and iron oxides as well as magnesia. The molten iron slag is first quenched in water or steam, which results in a glassy granular product. This product is then dried and milled into a fine powder, which can be used in concrete with ordinary Portland cement, and in combination with other pozzolanic materials. GGBS enhances the durability of concrete structures, by reducing the risk of damage caused by alkali-silica reactions and giving higher resistance to chloride penetration and to attacks by sulphate and other aggressives. [21]

A study by Malagavelli [21] on the effect of GGBS in normal concrete, shows that up to 50% of the cement can be replaced by GGBS without it affecting the compressive strength negatively. Yazici [22] shows in his studies that GGBS replacement has positive effects on the flexural behaviour of reactive powder concrete (RPC). The reason for this is an improvement in the binder phase, which in turn improves both the compressive strength and bond strength between the matrix and fibres. SEM investigations in these studies revealed the dense microstructure.

Rice Husk Ash

Rice husk is the hard covering protecting the rice grains, and is an agricultural waste from milling rice paddy. The rice husk is used as a fuel in the milling industry or as a fuel for power generation. When the rice husk is burnt in boilers, rice husk ash is produced. The ash

is about 25 weight-% of the rice husk, and it's estimated that 70 million tonnes are produced every year, worldwide. [23]

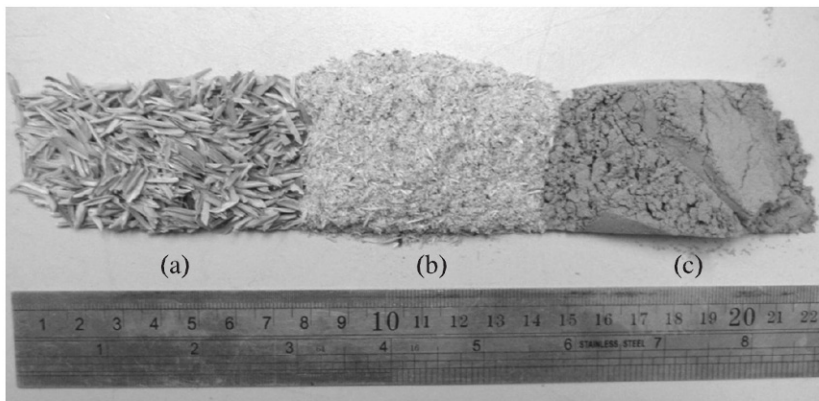


Figure 8 a) Rice husk, b) Burnt RHA and c) RHA after grinding [24]

Rice husk ash (RHA) is similar to silica fume in that way that it has a large specific surface area, and has a high content of amorphous silica. Compared to silica fume, which has spherical particles, RHA has angular and porous particles, see Figure 9. The average size can vary from 5 – 95 μm , and it has a BET surface area higher than 250 m^2/g . RHA can replace SF successfully with respect of durability of the concrete and compressive strength. [25, 26]

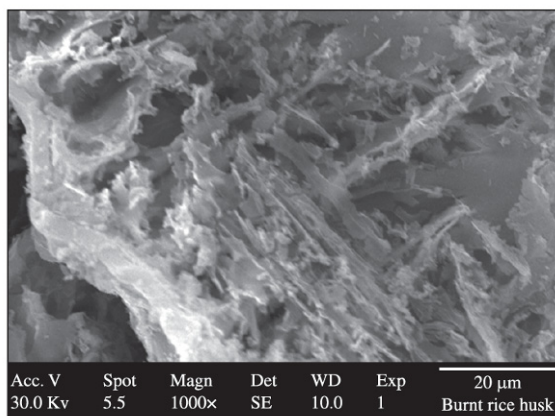


Figure 9 SEM for RHA particle [24]

In a study performed by Van Tuan et al [27] it was shown that RHA has good properties in reducing the autogenous shrinkage of UHPC. RHA has a very special porous structure, and affects both the rate and extent of hydration when added to cement. In addition to the shrinkage reducing effects, RHA also shows good pozzolanic properties like SF, because of its high silica content. Van Tuan's study shows that shrinkage is decreased with higher added amounts of RHA, whereas shrinkage increase with increased amounts of SF added.

In another study by Van Tuan et al. [28] it is shown that the addition of RHA in UHPC does not significantly decrease the compressive strength compared to that of SF. The RHA also has a fineness with a more favourable effect on compressive strength than SF.

The mean particle size of the RHA can be of importance regarding material properties in a concrete mix, as demonstrated by Van et al [29]. They found that a mean particle size of 7.41 μm (compared to sizes of 9.65, 6.22, 5.78 and 5.34) was the most suitable for producing an economical UHPC, where all silica fume was replaced by RHA. In the same study, the optimum content of replacing cement with RHA was considered to be 22.5 vol-%. [29]

Also Givi et al [26] have performed a study on how the particle size of RHA affect the concrete properties. The results showed that cement could be replaced by RHA up to a maximum limit of 15 % and 20 % with an average particle size of 95 and 5 μm , respectively. However, the optimal level of cement replaced by RHA for these two sizes was found to be 10 %. Similar results were found by Hebeeb and Mahmud [24].

Nanosilicas

Nanosilicas can contribute to denser packing of the matrix, because they are small enough to fill the voids between cement and SF particles. The denser matrix will have a higher content of C-S-H, which improves both the mechanical properties and the concretes durability [30]. Qing et al [31] performed tests to compare nano-SiO₂ addition's properties on hardened cement paste with those of SF. Their investigations showed that the pozzolanic activity of nanosilicas is much greater than that of SF. It makes the cement paste thicker and speeds up the hydration process of the cement. The bond strength between cement paste and aggregates was higher for mixes that contained nanosilicas than to mixes containing SF or the control mix with cement as the only binder.

In recent years two kinds of synthetic amorphous nanosilicas have attracted large research effort [32]. The two types of nanosilicas are:

- 1) Pyrogenic nanosilicas, whose particles can fuse together to form aggregates during the production process. These aggregates can also bind together and form agglomerates. Pyrogenic nanosilicas are commercially available as an effective filling agent.
- 2) Nanosilica sols, manufactured through polymerisation of silicic acid. They are almost monodispersed particles and do not form aggregates and agglomerates.

The two kinds of nanosilicas have similar specific surface area, but their different state with respect to agglomeration can influence their performance. By comparing the properties of one of each kind, Madani [32] found that pyrogenic nanosilica had faster pozzolanic reactivity as well as showing a higher hydration degree in cement pastes. [32, 33]

Special cements and the effects of combining binders

In literature, examples of special cements have been found, where ordinary cement is combined with different pozzolans. The aim seems to be to make a ready-mixed cement, with a smooth grain distribution and following a high packing density. This is important for UHPC because due to the very low w/c-ratio, the binder components cannot hydrate completely and have to work as fillers. However, using SF to fill the voids between the cement particles, large amounts of SF is necessary, typically between 10-30 % of the cement

mass. This is due to the size difference between cement and SF, see Figure 10. By using pozzolans with different sizes, the packing density can be optimized.

The following examples on special cements are collected from the article *Special cements for ultra-high performance concrete* [34].



Figure 10 To fill the voids between the cement particles, a larger amount of silica fume is needed [34]

1) Premium cements with Mikrodur technology

It is possible to design high performance concretes with modified cement and without silica fume. Dyckerhoff produces Mikrodur, which is a micro-fine cement made from Portland cement and blast furnace slag being milled and separated individually. The product has a constant grain distribution, see Figure 11. The micro-fine particles accelerate the hydration process whereas microfine particles of blast furnace slag leads to higher strength in the end and extend the concretes durability.

There are three different types currently available: F, U and X. By mixing F, U or X with OPC, specific properties can be precisely created.

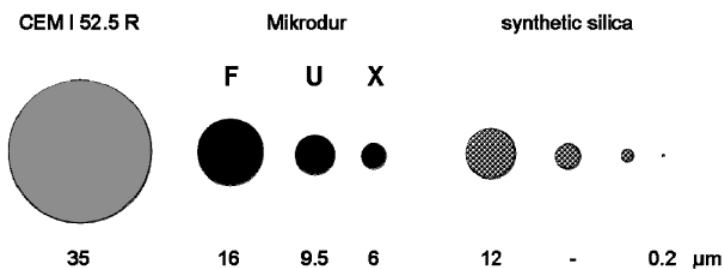


Figure 11 Particles to achieve a nearly continuous grain size distribution [34]

2) New cement with nanoscale synthetic pozzolans - Nanodur

The particle distribution is not continuously graded when using ordinary cement and silica fume. A nearly continuous grain size distribution can be achieved using OPC, microfine cements and industrially produced nanoscale synthetic silicas, see Figure 12.

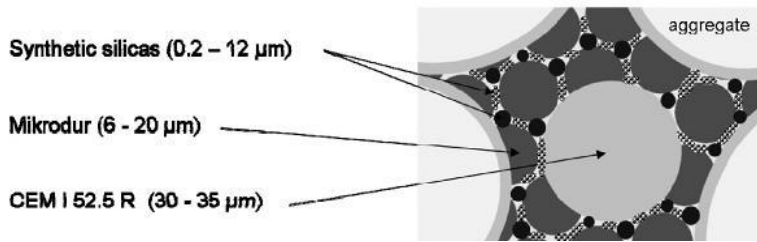


Figure 12 Dense packing of reactive binder components [34]

The synthetic SiO_2 particles runs much faster compared to silica fume [34]. Cements mixtures containing microfine clinker particles in combination with nanoscale synthetic silicas can therefore accelerate the hydration process. Microfine grains of blast furnace slag together with nanoscale synthetic silicas extend the durability of concrete.

Combining GGBS and FA have positive effects on compressive strengths compared to replacing cement with FA alone. Also, ternary blends of SF, FA and GGBS may be preferred over binary blends of SF and FA. This means that SF content can be reduced without losing the mechanical performance of the concrete. Reducing the amount of SF has been shown to reduce the amount of SP needed, resulting in an important environmental benefit. Using a ternary blend and thereby reducing the amount of cement will also decrease the heat of hydration and shrinkage as well as production costs. [22, 35]

Combining RHA and FA can improve both compressive strength and self-compactability of Self-compacting High performance Concrete[25]. The combination of SF and RHA makes it possible to replace the amount of cement with 40 % in UHPCs [28].

When RHA was combined with GGBS in a ternary binder composed of 65 vol% cement, 15 vol% RHA and 20 vol% of GGBS, a compressive strength of 165.2 MPa at 28 days was obtained. This was considered to be the optimum mixture proportions for the highest compressive strength.[29]

Several advantages could be achieved by making a premixed cement consisting of an OPC comprising microfine portland cement clinker, blast furnace slag grains and different synthetic silicas. First, it would ensure easy handling, dosage and homogeneity even with short mixing times. Second, a really dense packing of reactive binder components would be achieved. It seems likely that this would make the UHPRFC production, perhaps also in ready mix plants, much easier.

3.3 Aggregates

Aggregate size

It is important that the aggregates used in UHPFRC have a total grain size distribution which arrange a high packing density [16]. The largest fractions of the aggregate have traditionally been removed. The mean particle size is often below 1 mm, but aggregates up to 8 or 16 mm have also been used to produce UHPFRC [5]. If the maximum aggregate size is approximately 0,5 mm, one may use the term reactive powder concrete (RPC)[16]. It is essential that the aggregate has a high mechanical strength to prevent the aggregate to become the weak part of the concrete [2]. Examples of aggregate with very high strength can be calcined bauxite or granite.

When adding coarse aggregates to a mortar, the cement content is reduced, and therefore also the autogenous shrinkage and the price of the material are reduced. The use of coarse aggregates in UHPFRCs is scarce, but possible if the thickness of the constructional element is much larger than the aggregates[36]. Yang et al shows in [37] that UHPFRC used with coarse limestone aggregate can reach flexural strengths of 10 MPa. The concrete also showed good durability properties in terms of permeability and shrinkage.

Often, expensive silica sands are used in UHPFRs. However, silica sand can normally be replaced by natural sand, while still maintaining good mechanical performance and ductile behaviour. The use of natural sand does not necessarily influence the strength of UHPFRC significantly.[38]

It has been shown by Yang et al [38] that using recycled glass cullet for fine aggregates in UHPFRC gave promising mechanical properties compared to normal concrete, although it does not produce as high properties as natural sands. A possible explanation for this may be the lower bulk density achieved, resulting from grading of the material or particle shape. This can be resolved by modifying the grading in the recycled crushing process which would increase energy costs. Still, one also should consider the environmental and cost effects in producing a better UHPFRC using a recycled product, which most likely will be significantly attractive.

Recently more investigations are conducted on how to produce good UHPFRCs with commercially available materials. This is treated in chapter 3.7

3.4 Super-plasticizers

Due to the low w/b ratio, the use of superplasticizers is crucial to achieve a concrete which has a sufficient workability. A large quantity, which means up to 5 mass-% of the cement, is required [16]. The development of UHPFRC could not have happened without a development of SP additives. Only the third generation of plasticizers (polycarboxylate ethers, PCE) allow to save a sufficient amount of water to make the concrete workable [9].

3.5 Fibres

How fibres work

Ultra-high performance concretes are highly brittle, and the "performance" part of its name relies in fact on the addition of fibres. Fibres are therefore added to UHPCs to enhance the ductility of the material, in both tension and compression. The fibres increase the tensile and flexural strength of the concrete, while the fibres' contribution to the compressive strength is rather modest.

Rossi [1] thoroughly explains the role of the fibres in light of the cracking process. He divides between material and structural properties when looking at fibres in UHPFRC. The cracking process is described as following:

- Micro-crack: A crack with a length considered to be very small compared to the size of the specimen (structure).
- Macro-crack: A crack that must be considered **not** very small compared to the specimen or structure.
- Active crack: a crack that is having a normal or tangential displacement.
- Critical active crack: A crack that leads to a concentration of stresses and a localisation of strains, inside the specimen.

This means that cracking starts as behaviour of the material, and develops into behaviour of the structure.

When workability is not of importance long fibres can work on both micro-cracks and macro-cracks, or rather, at both the scale of the material and the structure. This applies to for example dry roller-compacted fibre-reinforced concretes. [1] From experiments, it is known that there is an upper limit for the amount of long fibres that can be added to the concrete without affecting workability excessively. However, dependent on concrete type and application, the fibre content can vary significantly. When the workability is of importance, the fibres added to the concrete are normally a mix of a larger amount of short fibres and a smaller amount of long fibres. This is the case of poured, pumped or sprayed concretes. [1]

When speaking of "long" or "short" fibres, and the amounts needed of each type, one must consider the *effect of scale*. The geometry of the structure and the type of stress will have an impact on the crack opening. The given size of fibres that is effective on the crack opening for this structure may not be effective for a larger structure. Also the largest diameter of the aggregate particles is of importance, as well as the mechanical characteristics of the matrix.

In a highly compact matrix that bonds well with the fibre, even a fibre considered to be short can function on a structural level. [1]

Choosing the fibres

The amount of fibres added to a concrete mix is measured as a percentage of the total volume of the composite (concrete and fibres) termed volume fraction (V_f). The fibres slenderness or aspect ratio (l/d) is calculated by dividing fibre length (l) by its diameter (d). Another way to characterize and compare the properties of different fibre reinforced concretes, is by using the so called “fibre factor”. [39]

$$\text{Fibre factor} = V_f \cdot \text{aspect ratio} = V_f \cdot l/d \quad [39]$$

The commonly use of steel fibre would probably be due to the many favourable properties of this fibre type: High modulus of elasticity, high strength, high ductility and a very good durability in the alkaline environment of the concrete. Failure will normally be characterized by a bond failure between the fibre and the surrounding matrix, due to their limited aspect ratio. [16]

type of fibre	unit weight [kg/dm ³]	tensile strength [MPa]	modulus of elasticity [GPa]	strain at fracture [%]	alkali resistance [-]	max. temperature [°C]	diameter [µm]
steel	7.8	500-2600	200	5-35	high	1000	100-500
alkali-resistant glass	2.6	2000-4000	75	20-35	med./low	800	12-20
carbon	1.75-1.91	2000-4000	200-450	4-15	high	3000	15
polypropylene	0.98	450-700	7.5-12	60-90	high	150	50
polyvinyl alcohol	1.3	800-900	26-30	50-75	high	240	13-300
polyester	1.4	800-1100	10-19	8-20	med.	240	10-50
aramide	1.42	700-3600	70-130	21-40	med.	600	12

Figure 13 Physical and mechanical properties of selected fibres for use in the production of fibre-reinforced concrete [16]

Inside the concrete, the steel fibres are protected against corrosion by the alkaline environment. Closer to the surface where the concrete may be carbonated, steel fibres may corrode in the presence of moisture. Then again, experiences have shown that the corrosion product around the fibres is not sufficient to build up enough bursting pressure to cause spalling of the concrete. This is due to the slenderness of the fibres. Even though the corrosion does not cause any significant damage from a safety perspective, the surface may be discoloured from the rust which from an esthetical point of view could be a problem. [16]

In ordinary fibre reinforced concretes, the length of the steel fibres varies in general from 12.7 mm to 63.5 mm, while the aspect ratio lies between 20 and 100. The most common diameters are in the range of 0.45 to 1 mm [40]. The usual amount of steel fibres lies between 0.25 vol-% (20kg/m³) to 2 vol-% (157 kg/m³) [40]. In UHPFRCs on the other

hand, the fibres can be smaller than 12 mm, and the total content can be as high as 11 % by volume [6]. However, according to [16] it has been proven that approximately 2.5 vol% of steel fibres at an aspect ratio l/d between 40 to 60 leads to the best results, both in view of fresh and hardened concrete properties.

To ensure a low porosity, it should be noted that the fibres length should be adjusted to the maximum aggregate diameter. This is illustrated in Figure 14. For RPC, where the maximum grain size is approximately 0.5 mm, the fibre length should at least be equal to ten times the maximum aggregate diameter [16].

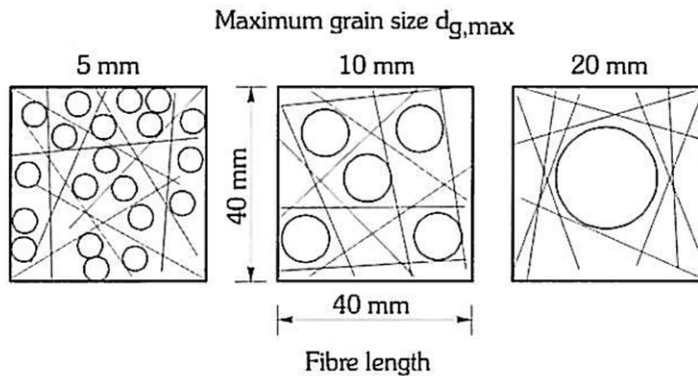


Figure 14 Influence of d_{max} on fibre distribution [41]

3.6 Production methods

Workability

Based on experience with conventional fibre reinforced concrete, one might expect challenges related to the UHPFRCs workability. However, this seems not to be a common problem according to the literature review. On the other hand, UHPFRC is not workable without the addition of large quantities of high performance plasticizers, i.e up to 5 mass% of the cement [16]. In some of the reviewed articles, use of air-entraining agent is stated [42]. It is known that this type of addition may result in improved workability, in addition to increased frost resistance [16].

Addition of fibres increases the amount of water required for the concrete mix [16]. Also, problems due to formation of “fibre nests” can occur [42]. The fibre aspect ratio l/d has a critical influence when it comes to the ability of the fibres to be mixed into the concrete, and the concrete's workability. In general, the workability decreases as the aspect ratio increases.

Mixing

The production of UHPC (and also SCC) can require long mixing times, which again cause capacity reduction on production plant, as well as increases of cost significantly [43]. Investigating how mixing times of UHPC can be reduced [43], the following measures were found effective:

- Increase speed of mixing
- Optimize particle size distribution by replacing cement and quartz flour with SF, and thereby increasing the relative solid concentration
- Match the type of superplasticizer with the cement used.

The mixing sequence and type of mixer are also factors that can affect the concrete, in addition to mixing time. Chang and Peng [44] found that for HPCs the following was true:

- Under high binder content ($N > 1.8$) the mixing sequence and type of mixer have less impact on the uniformity of the concrete, given sufficient mixing time.
- Under low binder content ($N > 1.6$) the effect of mixing sequence and type of mixer on mixing efficiency is more notable.

Curing conditions

Sometimes UHPFRCs are subjected to a thermal treatment. The reason for subjecting the concrete element to this treatment are the following benefits, outlined in [4]:

- The concrete strengthens faster (compressive and tensile strengths)
- The concrete experiences a reduction in delayed shrinkage and creep effects
- The durability of the concrete is substantially improved

The heat treatment initiates the formation of more hydrates, which give the raise to the improved characteristics [45].

Simon [45] identifies two types of heat treatment:

- 1) Autoclaving at a moderate temperature normally limited to 65°C because higher temperatures alters the risk of delayed ettringite formation, and with high humidity. This procedure mainly reduces the early setting time.
- 2) Concrete that has been removed from its form hours before is put in an enclosure where the temperature is gradually raised to approx. 85-90°C. The concrete is kept at that temperature and a relative humidity close to 100% for one or two days. Because this treatment is applied after the concrete has set it is essential to have knowledge about the concretes setting time [4]. This kind of treatment will affect the concretes material properties due to the formation of more hydrates in the concrete. The concrete will have improved certain aspects of durability, better long-term mechanical performance and reduced shrinkage and creep after the treatment.

[2, 4]

Heinz et al [46] show in their experiments that the exact conditions for heat treatment should be optimised for every particular UHPC. Concrete containing GGBS and OPC required a longer initial storing period before treatment or a longer heat treatment to gain higher strength, compared to concrete containing only OPC or OPC and FA.

Ipek et al have done studies on the effect of applying pre-setting pressure on RPC during the setting phase. In [47] different pressures were applied, and the specimens were subjected to thermal treatment during the curing phase. A pressure of 25 MPa doubled the compressive strength of the specimens, and it was seen that this pressure was sufficient to reduce large air spaces and free water in the samples considerably. In [48] it is shown that a pre-setting

pressure of 5 MPa is the most effective with regards to improving the flexural strength. An increase of 34 % was obtained.

Even though heat-curing is an effective way to enhance material properties of UHPFRC, it is costly and energy-consuming. It limits the production of UHPFRC to the precast-industry, and hence also restricts the use of the material. [38]

3.7 UHPCs with commonly available materials and/or technology

A factor challenging the wide scale use of UHPC is the availability of raw materials. The majority of reference projects where UHPC is used are based on prebagged (commercially available) materials, which comes with cost and logistics issues. To widen the use and make the use of the material more attractive, the use of local available materials can be the solution. Developing UHPFRCs without heat or pressure treatment would also encourage utilisation of the material, but has been quite challenging for a long while due to all the influencing parameters. [15, 49]

Using local materials from the south of Norway, and the packing programme EMMA, UHPFRCs with compressive strengths between 160-190 MPa (heat cured), and flexural strengths above 20 MPa (with 2 vol% fibres) have been made. The UHPCs also showed excellent chloride resistance. [15, 50]

Wang et al [51] concludes in their study that UHPC can in fact be produced with common technology and without removing the coarse aggregate. They used extremely low W/b ratio, high binder content including multi-addition of SF, GGBS and limestone powder, and a high standard super-plastiziser. They achieved high compressive strengths even when curing at room temperature, and can also conclude that pumpable UHPC can be produced with the help of super-plastiziser and retarder in combination.

Camacho et al performed a study [36], seeking to develop VHPFRC-UHPFRCs suitable for production in precast companies without the need to adapt special mixing/curing processes, and by using local materials that are normally used to produce normal concretes (in this case limestone coarse aggregates). Their results are shown in Figure 15.

Type	Cement	Addition	W/B	Coarse Aggregate	Long Fibers	Mixer	Compr-Flex strength expected
Level	Kg/m ³	%o.c.w.	Ratio	Kg/m ³	Tensile strength	Type	MPa-MPa equiv.
Basic	522	10%	0,27	600	>1200	Low Energy	120-15
Medium	850-635	10%	0.21	0-600	2000	LE-Intensive	135-28
High	1000	15%	0.175	0	2000	Intensive	160-35

Figure 15 Dosage of three different performance VHPFRC-UHPFRCs [36]

Wille et al [49] describes a research where UHPC with compressive strength up to 190 MPa without fibres and exceeding 200 MPa with fibres was obtained. For the mix design only materials commercially available in the US was used.

3.8 Examples of UHPFRCs mix design

Common commercially available UHPFRCs

Most UHPC-UHPFRCs experiences have been developed in France, Germany, Denmark, Japan and USA. Camacho et al [36] sums up the mix design for some of the commercially available products.

	Ductal®		BSI®		CRC®		CEMTEC ^{multiscale} ®		BCV®	
	Type	kg/m ³	Type	kg/m ³	Type	kg/m ³	Type	kg/m ³	Type	kg/m ³
Cement	Portl.	746	-	1114			CEM I 52.5	1050		↑
Silica fume	-	242	-	169	Binder	930	-	275		2115
Quartz flour	-	224	-	-			-	-		premix
Sand (mm)	0,1-0,6	1066	0-6	1072	0-5	1325	<0,5	730	2-3	↓
Water	W/C	0,19	W/C	0,19	W/B	0,16	W/C	0,181	W/C	0,25
Admixture	Chryso	9	SIKA	40	-	-	Chryso	35	-	21.5
Fiber	13/0.2	161	20/0.3	234	12/0.4	150-300	10/0.2	470	20 _{2/3} 13 _{1/3}	156
SlumpFlow(mm)		700		640		-		-		750
f _{ct,28} (MPa)		8		8.8		-		-		8
f _{cm,7} (Mpa)	20°	101	20°	165		-	20°	-	20°	98
f _{cm,28} (Mpa)	20°/90°	124/198	20°	199	20°/90°	150/400	20°	168	20°/90°	130-150

Figure 16 Dosages and properties of the most common commercial UHPFRCs [36]

Examples of some UHPFRCs from literature

Type	UHPC				UHP-FRC				SIFCON
	A ^d	B ^d	C	D	A ^d	B ^d	C	D	
Cement	1.00	1.00	1.00	1.00	1.00	1.00	1.00	1.00	1.00
Silica Fume	0.25	0.25	0.25	0.25	0.25	0.25	0.25	0.25	0.25
Glass Powder	0.25	0.25	0.25	0.25	0.25	0.25	0.25	0.25	0.25
Water	0.220	0.195	0.190	0.180	0.212	0.200	0.185-0.195	0.18-0.20	0.207
Superplasticizer ^a	0.0054	0.0108	0.0108	0.0114	0.0054	0.0108	0.0108	0.0108	0.0108
Sand A ^b	0.28	0.30	0.31	1.05	0.27	0.28	0.29	0.92	0.76
Sand B ^c	1.10	0.71	0.72	0.00	1.05	0.64	0.67	0.00	0.00
ratio Sand A/B	20/80	30/70	30/70	100/0	20/80	30/70	30/70	100/0	100/0
Fiber	0.00	0.00	0.00	0.00	0.15/0.25	0.22	0.18-0.27	0.22-0.31	0.71
Fiber Vol.%	0	0	0	0	1.5/2.5	2.5	2.0-3.0	2.5-3.5	5 ^e /8 ^f
f' _c [cube,28d] MPa	194	207	220-240	232-246	207/213	219	227-261	251-291	270 ^g /292 ^f
f _t [tension] MPa	6.1-7.4 ^g	6.9-7.8 ^g	7.4-8.5 ^g	8.2-9.0 ^g	8.2/14.2	15	16-20	20-30	37 ^e

^a solid content; ^b max. grain size 0.2 mm (1/128 in.); ^c max. grain size 0.8 mm (1/32 in.);

^d non vibrated, non surface cut; ^e twisted (T) fiber; ^f straight (S) fiber; ^g at first cracking followed by immediate failure

Figure 17 Examples of mixtures developed for UHPC and UHPFRC [8]

Material	Amount (kg/m ³ (lb/yd ³))	Percent by Weight
Portland Cement	712 (1,200)	28.5
Fine Sand	1020 (1,720)	40.8
Silica Fume	231 (390)	9.3
Ground Quartz	211 (355)	8.4
Superplasticizer	30.7 (51.8)	1.2
Accelerator	30.0 (50.5)	1.2
Steel Fibers	156 (263)	6.2
Water	109 (184)	4.4

1 kg/m³ = 1.686 lb/yd³

RDM = relative dynamic modulus (see p. 134)

Figure 18 Typical UHPC Composition from Graybeal [52]

Type	UHPC	UHP-FRC	SIFCON
Cement	1.00	1.00	1.00
Silica fume	0.25	0.25	0.25
Glass powder	0.25	0.25	0.25
Water	0.180	0.18 to 0.20	0.207
High-range water-reducing admixture*	0.0114	0.0108	0.0108
Sand A†	1.05	0.92	0.83
Fiber	0.00	0.22 to 0.31	0.49
Fiber, vol. %	0	2.5 to 3.5	5.5
f_c' , MPa‡	232 to 246	251 to 291	270
f_t , MPa§	8.2 to 9.0†	20 to 30	37

*Solid content

†Maximum grain size 0.2 mm

‡28-day tests using 50 mm cubes

§At first cracking, followed by immediate failure

1 MPa = 145 psi; 1 mm = 0.04 in.

Figure 19 Mix proportions by weight, from Wille, Naaman and El-Tawil

4 Material properties

4.1 Mechanical properties

Compressive strength

As the name indicates, UHPFRCs have compressive strength much higher than ordinary concretes. The typical compressive strength of UHPC is in the range of 150 – 220 MPa, but higher strengths can be obtained. Adding fibres would in general have a low influence on the compressive strength, but it would considerably affect the stress-strain behaviour. Up to 70 - 80 % of compressive failure load, the concrete exhibit an elastic behaviour. This is illustrated in Figure 20. [53]

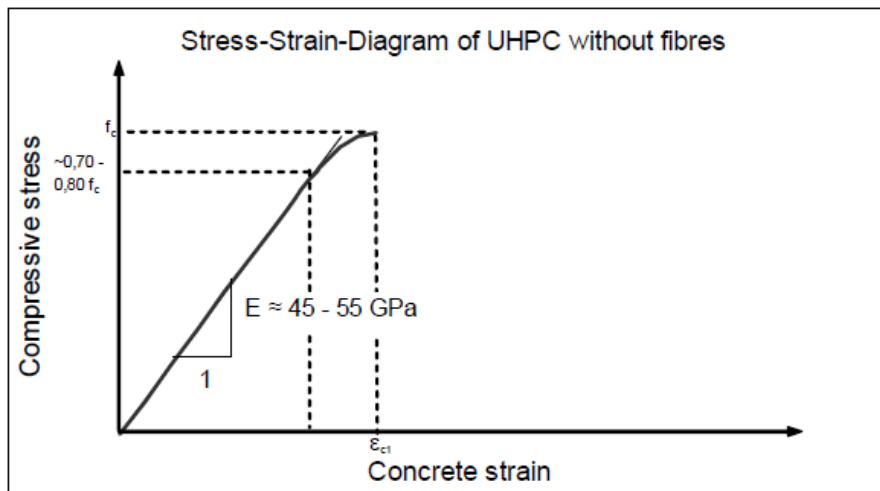


Figure 20 Stress-strain diagram of UHPC [53]

UHPC with and without fibre reinforcement behaves very differently when exposed to compressive strength. While UHPC without fibre reinforcement exhibit a very dramatic and brittle failure, which can be described as an explosion, UHPFRC exhibit a very ductile failure, see Figure 21. This is due to the restraining and confining effects of the fibres[54].

The slope of the descending branch depends on [53]:

- fibre content
- fibre geometry (length, diameter)
- fibre length in relation to maximum aggregate size
- fibre stiffness (in case of fibre cocktails)
- fibre orientation

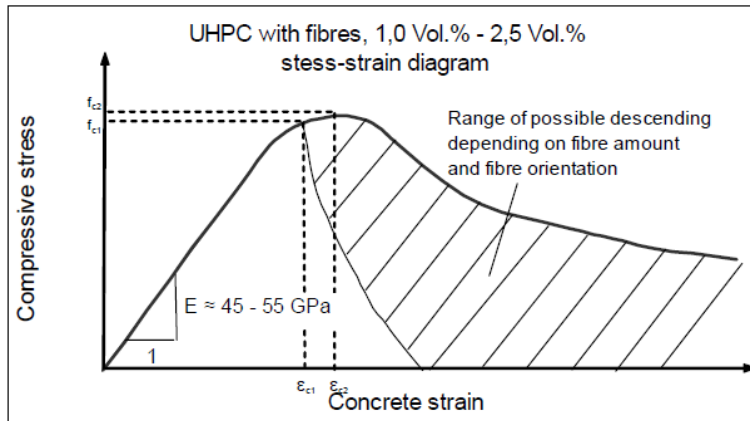


Figure 21 Stress-strain diagram of UHPFRC [53]

Further, the mechanical strength is influenced by several parameters described throughout this report, especially the packing density, curing conditions and aggregate. Tests on one type of UHPFRC, CRC, showed a compressive strength at around 150 MPa when using quartz sand and curing at ambient temperature. To achieve a higher strength, special aggregate like bauxite was necessary. When combining this with heat curing, the compressive strength could be as high as 400 MPa.[55]

Experiments [54] show that the set time of UHPC is clearly delayed compared to normal concrete. The final set may not occur until 12-24 hours after casting, and this time could also be longer, depending on the admixtures in the concrete mix. When set finally occur, UHPC gains its compressive strength rapidly.

According to AFGCs recommendations compressive strength should be determined on cylinders with dimensions F7x14 cm or F11x22cm. It is also possible to measure the compressive strength on cubes, according to Eurocode 2 [EC2], provided the coefficient for switching from cylinders to cubes during design or suitability testing has been validated [45]. Further details on test methods can be found in Annex 1, or in [4].

Tensile and flexural strength

High compressive strength is not always the most important feature of an UHPFRC; the flexural strength is often of higher importance [36].

Similar to other fibre reinforced concretes (FRC) UHPFRC can be classified as either “strain-softening” or “strain-hardening” in tension. Strain softening means that the maximum tensile capacity decreases after the crack opening. This is illustrated in Figure 22 and means that the fibres do not contribute to hold the cracks together. However, the fibres may increase the tensile strength beyond the matrix strength (i.e. a larger force is required before the concrete cracks). Without fibres, UHPC can exhibit a direct tensile strength in the range of 7 – 10 MPa. According to [16], the tensile strength may be doubled when fibres are added to the mix. The increase depends on the amount, type and orientation of the fibres. If the tensile capacity increases after cracking, the concrete exhibits a hardening behaviour. This is illustrated in Figure 23. In this case, the fibres stitch the concrete together when it cracks. Only a few materials are hardening in pure tension knowing that this requires a very high fibre content [56]. Some CEMTEC mixes which have fibre contents of around 11 % by volume (type 3, chapter 2.2), exhibit hardening behaviour [56].

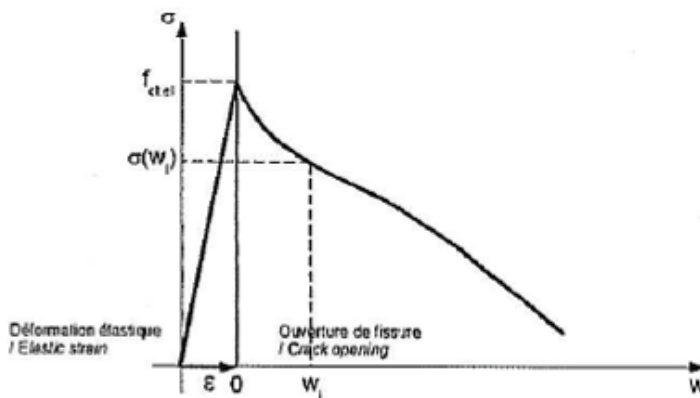


Figure 22 Strain-softening behaviour [45]

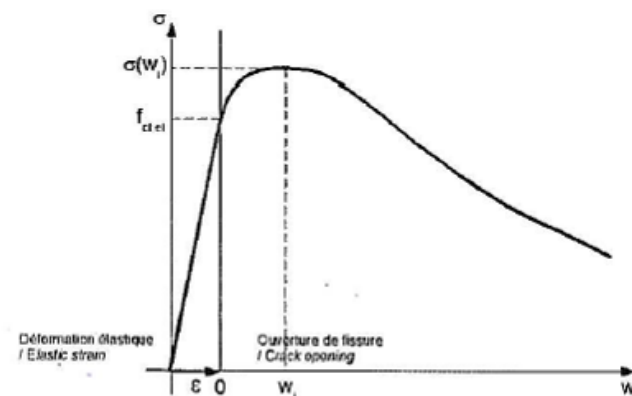


Figure 23 Strain-hardening behaviour [45]

The flexural strength of UHPFRC is usually much higher than the direct tensile strength. In [42] façade elements made of BCV (Composite Concrete Vicat), which is a type UHPFRC,

the flexural strength from 3 points bending test on notched specimens, was determined to be 16.4 MPa when the mix contained 1 % short fibres. For another mix with 2 % steel fibres by volume where 1/3 of the fibres were short and the rest long, the flexural strength was measured to be 23.1 MPa. A softening response was observed.

It should be pointed out, that even if an UHPFRC exhibit strain hardening behaviour in bending, it does not necessary mean that it exhibits strain hardening in direct tensile. Also, the fibre orientation and size of the test specimens influence greatly on the behaviour. Therefore, softening or hardening behaviour cannot be considered to be a material characteristic, but rather a structural constructional characteristic.

Based on recent research, the interim recommendations from AFGC identify three types of UHPFRC as determined by their direct tensile behaviour [45]:

- 1) Softening materials that have softening average law in direct tension
- 2) UHPFRC with a hardening average constitutive law in direct tension, but with a softening characteristic law
- 3) UHPFRC with a hardening characteristic constitutive law in direct tension

This means that if one, for example, have three test specimens which are tested, and two of them exhibit strain-hardening behaviour while the last specimen exhibits strain softening behaviour, the average behaviour in tensile could be hardening. However, when calculating the characteristic value, the uncertainty related to the tensile strength after the concrete cracks, is much larger than before it cracks. As a result, the characteristic behaviour in tensile may be softening.

Category 1 contains UHPFRCs with a low fibre content which generally does not respect the non-brittleness criterion required for structural concrete. Category 2 is the case most commonly encountered currently with UHPFRCs like Ductal, BSI etc., while pure strain hardening behaviour requires UHPFRCs with a very high content of fibres. An example can be certain CEMTEC mixes which have fibre contents of around 11 % by volume [45].

The literature seems to be a bit inconclusive on how to test the flexural, and especially the direct tensile, strength of UHPFRC. This includes a lack of design codes and analytical tool, especially in the U.S.[57]. Association Française de Génie Civil (AFGC) and Service d'études techniques des routes et autoroutes (Setra) published their interim recommendations on UHPFRC in January 2002[4], and an updated version in to be published in 2012. In addition, the U.S Federal Highway Administration and the French IFSTTAR has established a joint research that according to [58] has succeeded in advancing the field of flexure testing. They also have developed a new and more practical direct tension test method.

Further details on test methods can be found in Annex 2 and 3, or in [4] and [58].

The mechanical properties of air-cured UHPFRC at early ages has be studied [59], and also a model to predict them has been proposed based on the test results by Hong et al. The flexural strength was tested with unnotched specimens in a three-point bending test. The study concludes that the flexural strength manifested itself rapidly up to the age of 3 days, and the strength at 7 day was almost the same as the strength at day 28. The study also included a

comparison of flexural strength with heat-cured specimens. The results showed only a difference of 11 %, and conclude that heat-curing has only a very small effect on flexural strength.

Fibre orientation has been shown by Kang [60-62] to be important for the flexural behaviour of UHPFRC. From bending tests it was found a linear increase between flexural tensile strength and fibre volume ratio. The initial cracking seems to be little affected by both orientation and distribution of the fibres. The flexural strength on the other hand, is highly influenced by the fibre orientation. The fibre orientation is determined by the placing direction of the concrete, and concretes placed parallel to the longitudinal direction of the specimen showed considerably higher flexural strength.

Impact strength

When concrete is subjected to an impact it experiences high rates of localised strain. High rates of strain cause an increased compressive and tensile strength. UHPFRC has, like most fibre-reinforced concretes a high energy dissipation capacity. Also, because of its large tensile strength, the cracking and structural integrity can be controlled. This holds true even for quite strong impacts. [4]

Investigations on an UHPFRC with at least 50 % of the OPC replaced by FA, slag and SF, and natural sand as fine aggregates was done to see how single and multiple dynamic impacts will affect the concrete [63]. The experiments were done with different volume fractions of steel fibres. The results showed that addition of steel fibres will enhance that concrete's resistance against repeated dynamic impacts; the dynamic strength, deformation and energy absorption are largely influenced. The investigations conclude with the following:

- The number of impacts the concrete can withstand increases sharply with increased volume fraction of steel fibres
- The energy absorption increases linearly with addition of steel fibres
- Adding steel fibres to the concrete can prevent disruption and hence maintain the integrity of the specimen.

According to Leonhardt [64] a higher ductility of the UHPFRC improves the impact resistance, and therefore knowledge of optimum fibre content and fibre orientation is crucial. Results have shown that the impact resistance was increased with the amount of micro steel fibres ($d=0.16$ mm). Higher horizontal fibre alignment increased the impact resistance. When 1.0 % of the micro fibres were replaced with crimped fibres with a larger diameter, impact resistance was reduced. This was due to a reduction in number of fibres in the mix, and hence a smaller deformation energy of the concrete.

4.2 Properties dependent on time and/or temperature

Shrinkage

UHPFRC experiences very low drying shrinkage and the reason may be the low porosity. Studies on shrinkage have shown that no drying shrinkage was found if the UHPFRC produced without coarse aggregates[16]. Due to the large amount of cement in UHPFRCs, the autogenous shrinkage is large, and may reach values higher than 0.0012 (1.2 $\mu\text{m}/\text{mm}$). This is as expected, and most of the autogenous shrinkage takes place at the age 8 to 24 hours.[16]

Creep in compression

UHPFRCs show larger creep than one would expect when considering the strength of the material. For normal strength concretes, the creep coefficient will decrease as material strength increases. For UHPFRCs, final creep coefficients between 2 and 3 can be observed for loading at early age ($t_0 = 3$ days and $t_0 = 1$ day, respectively). The reason for this behaviour is the large amounts of paste in these concretes.[16]

Heat treatment will reduce creep significantly, and a heat treated UHPFRC will not experience any more shrinkage[4]. A study performed by Flietstra et al [65] shows that the effects of thermal treatment performed under a compressive load "locks in" the creep strains in the concrete, independent of when during the early age (28 days) the treatment is performed. A study by Graybeal [52] showed that heat and steam treatment caused a decrease in creep coefficient. Also Garas [66] show that compressive creep is significantly decreased by thermal treatment.

Tensile creep

Often when we talk about creep we actually refer only to creep in compression. Creep also occurs in tension, and results [66] show that creep in UHPC is quite different in tension and compression. It is put emphasis that further study of tensile creep is needed for UHPC. This is especially true for applications where a high long-term tensile performance is important. Garas et al [66] investigated the effect of thermal treatment on tensile creep, and provided some interesting findings:

- Tensile creep of UHPC seems to be more susceptible to thermal treatment than tensile strength.
- Microcracking and porosity is proposed to significantly affect tensile creep of UHPFRC. It is however pointed out that further research is needed to more thoroughly describe the factors influencing the tensile creep behaviour.

4.3 Durability

Permeability

The durability of a concrete is largely linked to permeability of the material. Because of the high rate of autogenous shrinkage in UHPFRC, micro-cracks will form and the result is a concrete with reduced resistance against penetrating aggressives. Micro-cracks can also be a result from thermal treatment. Scheydt and Müller [67] shows that the interfacial transition zone (ITZ) that forms between the cement paste and coarse aggregates or steel fibres can decrease the concrete's durability.

Still regarding the risk of microcracks reducing the durability, studies show that UHPFRC has good durability properties. Graybeal [52] confirms through a large study that the durability properties of UHPC are significantly better than those of normal concrete. Also Toledo Filho et al [68] show this in their study. They used probabilistic analysis and found that the cover thickness of their UHPFRC could be a factor of 10 less than for ordinary concrete, and still maintain the same level of protection of the reinforcement bars. They conclude that UHPFRC is a suitable material for surface protection and/or impermeable situations, especially under extreme conditions. Area of application can be in roads, marine structures or nuclear power plants.

Elevated temperature/fire

A rapid increase of temperature can lead to the risk of spalling in concrete. This holds especially true for high-strength concrete and the spalling can be explosive. Such concrete has low porosity and the vapour pressure that builds up inside the concrete cannot easily be released. Concrete's resistance to fire is a widely investigated topic, and Pimienta et al [69] tries to sum up results from fire tests performed on some commercially available UHPFRCs, see Figure 24. [70]

Specimen geometry	UHPFRC	Thermal treatment	Fire curve	Applied load	Observation
Slabs 400 x 400 x 25 mm ³	Ductal®-AF	Yes ***	ISO 834	Unloaded	No spalling
		No			No spalling
	Ductal®-FM *	Yes			Spalling
Columns 900 x 200 x 200 mm ³ 700 x 300 x 300 mm ³	Ductal®-AF	Yes	ISO 834	Unloaded	No spalling
		No			Minor spalling
	Ductal®-FO **	Yes			Severe spalling
I shape beam Span = 6,15 m	Ductal®-AF	Yes	ISO 834	Loaded (4 points bending)	Minor spalling
		No			No spalling
Cubes 100 x 100 x 100 mm ³ Cylinders Ø 110 mm x h 220 mm	BSI®-fire	Yes ****	HC _{inc}	Unloaded	No spalling
		No			
U shape sample 1 500 mm [11]	CERIB UHPC I et II without pp fibres	No	ISO 834	Unloaded	Severe spalling
U shape sample 1 500 mm [11]	CERIB UHPC I et II with pp fibre	No	ISO 834	Unloaded	No spalling

(*) No pp fibres; (**) no pp fibres, with organic fibres; (***) 48 hours at 90°C; (****) 48 hours at 80°C, in sat. vapour.

Figure 24 Details of the tests in fire performed on Ductal®, BSI and CERIB-UHPC [69]

From their literature review some conclusions are drawn, even though the UHPFRCs examined show large variations in parameters such as compressive strength, elastic modulus and thermal strain:

- The compressive strength is a (highly) nonlinear decreasing function of temperature
- The elastic modulus also decreases with temperature, but in a more regular manner.
- Polypropylene fibres have shown good effects in limiting or preventing spalling behaviour.

The behaviour of UHPFRCs at high temperatures is highly complex, and the updated version of the French AFG-SETRA guidelines (to be published in 2012) considers the information gathered so far. [69]

References

1. Rossi, P., *Ultra-High-Performance Fiber-Reinforced Concretes*. Concrete International, 2001. **23**(12): p. 46-52.
2. Resplendino, J., *Introduction: What is UHPFRC?*, in *Designing and building with UHPFRC - State of the Art and Development*, F. Toutlemonde and J. Resplendino, Editors. 2011, ISTE ltd;: London. p. 3-12.
3. Habel, K., et al., *Development of the mechanical properties of an Ultra-High Performance Fiber Reinforced Concrete (UHPFRC)*. Cement and Concrete Research, 2006. **36**(7): p. 1362-1370.
4. AFGC and SETRA, *Ultra High Performance Fibre-Reinforced Concretes - Interim Recommendations*. 2002, Association Francaise de Génie Civil.
5. Habel, K., *Structural behaviour of elements combining Ultra-High Performance Fibre Reinforced Concretes (UHPFRC) and reinforced concrete*, in *Faculté Environnement naturel, architectural et construit - Institut de structures - Section de Génie Civil*. 2004, École Polytechnique Fédérale de Lausanne: Lausanne.
6. Rossi, P., *Ultra-High Performance Concretes*. Concrete International, 2008. **30**(02): p. 31-34.
7. Vogt, C., *Ultrafine particles in concrete*, in *School of Architecture and the Built Environment, Division of Concrete Structures*. 2010, KTH: Stockholm.
8. Naaman, A. and K. Wille, *The Path to Ultra-High Performance Fiber Reinforced Concrete (UHP-FRC): Five Decades of Progress*, in *Proceedings of Hipermat 2012 - 3rd International Symposium on UHPC and Nanotechnology for Construction Materials*. 2012, Kassel University Press: Kassel, Germany.
9. Deeb, R., A. Ghanbari, and B.L. Karihaloo, *Development of self-compacting high and ultra high performance concretes with and without steel fibres*. Cement and Concrete Composites, 2012. **34**(2): p. 185-190.
10. Smeplass, S., *Fresh concrete - proportioning*, in *TKT Concrete Technology I*, S. Jacobsen, Editor. 2009, NTNU: Trondheim, Norway.
11. Sellevold, E.J., *Pozzolans*, in *TKT 4215 Concrete Technology I*, S. Jacobsen, Editor. 2009, NTNU: Trondheim, Norway.
12. Okuma, H., et al., *The First Gighway Bridge applying Ultra high Strength Fiber Reinforced Concrete in Japan*, in *7th Internation Conference on Short and Medium Span Bridges*. 2006: Montreal, Canada.
13. Lagerblad, B. and K. Kjellsen, *Normal and high strength concretes with conventional aggregates*, in *Engineering and transport properties of the Interfacial Transition Zone in cementitious materials*. 1999, RILEM Publications.
14. Lowke, D., et al., *Control of Rheology, Strength and Fibre Bond of UHPC with Additions – Effect of Packing Density and Addition Type*, in *Proceedings of Hipermat 2012 - 3rd International Symposium on UHPC and Nanotechnology for Construction Materials*. 2012, Kassel University Press: Kassel, Germany.
15. Fidjestol, P., R.T. Thorsteinsen, and P. Svennevig, *Making UHPC with local materials - The Way Forward*, in *Proceedings of Hipermat 2012 - 3rd International Symposium on UHPC and Nanotechnology for Construction Materials*. 2012, Kassel University Press: Kassel, Germany.
16. fib, *Structural Concrete - Textbook on behaviour, design and performance*. Bulletin 51. Vol. 1. 2009, Lausanne: fédération internationale du béton (fib). 95-149.
17. Locher, F.W., *Classification of cements*, in *Cement - Principles of production and use*. 2006, Verlag Bau+Technik: Dusseldorf.
18. NPCA. *Fly ash - National Precast Concrete Association*. [cited 2012 28-04]; Available from: precast.org/tag/fly-ash.
19. FlyashAustralia. *Flyash Australia*. [cited 2012 28-04]; Available from: <http://www.flyashaustralia.com.au/WhatIsFlyash.aspx>.

20. Malhotra, V.M. and P.K. Mehta. *High-Performance, High-Volume Fly-Ash Concrete: Materials, Mixture, Proportioning, Properties, Construction practice and Case Histories*. 2002. Ottawa: Supplementary Cementing Materials for Sustainable Development Inc.
21. Malagavelli, V. and P.N. Rao, *High Performance Concrete with GGBS and ROBO Sand*. International Journal of Engineering Science and Technology, 2012. **2**(10): p. 5107-5113.
22. Yazıcı, H., et al., *Mechanical properties of reactive powder concrete containing high volumes of ground granulated blast furnace slag*. Cement and Concrete Composites, 2010. **32**(8): p. 639-648.
23. *ricehuskash.com*. 2012 [cited 2012 17 April].
24. Habeeb, G.A. and H. Bin Mahmud, *Study on Properties of Rice Husk Ash and Its Use as Cement Replacement Material*. Materials Research-Ibero-American Journal of Materials, 2011. **13**(2): p. 185-190.
25. Le, H.T., K. Siewert, and H.-M. Ludwig, *Synergistic Effect of Rice Husk Ash and Fly Ash on Properties of Self-Compacting High Performance Concrete*, in *Proceedings of Hipermat 2012 - 3rd International Symposium on UHPC and Nanotechnology for Construction Materials*. 2012, Kassel University Press: Kassel, Germany.
26. Givi, A.N., et al., *Assessment of the effects of rice husk ash particle size on strength, water permeability and workability of binary blended concrete*. Construction and Building Materials, 2010. **24**: p. 2145-2150.
27. Van Tuan, N., G. Ye, and K. van Breugel, *Mitigation of early age shrinkage of Ultra High Performance Concrete by using Rice Husk Ash*, in *Proceedings of Hipermat 2012 - 3rd International Symposium on UHPC and Nanotechnology for Construction Materials*. 2012, Kassel University Press: Kassel, Germany.
28. Van Tuan, N., et al., *The study of using rice husk ash to produce ultra high performance concrete*. Construction and Building Materials, 2011. **25**(4): p. 2030-2035.
29. Van, v.t.A. and H.-M. Ludwig, *Proportioning Optimization of UHPC Containing Rice Husk Ash and Ground Granulated Blast-furnace Slag*, in *Proceedings of Hipermat 2012 - 3rd International Symposium on UHPC and Nanotechnology for Construction Materials*. 2012, Kassel University Press: Kassel, Germany.
30. Ghafari, E., et al., *Optimization of UHPC by Adding Nanomaterials*, in *Proceedings of Hipermat 2012 - 3rd International Symposium on UHPC and Nanotechnology for Construction Materials*. 2012, Kassel University Press: Kassel, Germany.
31. Qing, Y., et al., *Influence of nano-SiO₂ addition on properties of hardened cement paste as compared with silica fume*. Construction and Building Materials, 2007. **21**(3): p. 539-545.
32. Madani, H., A. Bagheri, and P. Tayebe, *A comparison between the pozzolanic reactivity of nanosilica sols and pyrogenic nanosilicas*, in *Proceedings of Hipermat 2012 - 3rd International Symposium on UHPC and Nanotechnology for Construction Materials*. 2012, Kassel University Press: Kassel, Germany.
33. Shakhmenko, G., et al., *UHPC Containing Nanoparticles Synthesized by Sol-gel Method*, in *Proceedings of Hipermat 2012 - 3rd International Symposium on UHPC and Nanotechnology for Construction Materials*. 2012, Kassel University Press: Kassel, Germany.
34. Strunge, J., *Special cements for ultra high performance concrete*, in *Proceedings of the Second International Symposium on Ultra High Performance Concrete*, F.S. Stürwald, Editor. 2008, University of Kassel: Kassel, Germany. p. 61-68.
35. Yazıcı, H., et al., *Utilization of fly ash and ground granulated blast furnace slag as an alternative silica source in reactive powder concrete*. Fuel, 2008. **87**(12): p. 2401-2407.
36. Camacho, E., J.Á. López, and P. Serna, *Definition of three levels of performance for UHPFRC-VHPFRC with available materials*, in *Proceedings of Hipermat 2012 -*

- 3rd International Symposium on UHPC and Nanotechnology for Construction Materials*. 2012, Kassel University Press: Kassel, Germany.
37. Yang, J., et al., *Characteristics of Mechanical Properties of Ultra-high Performance Concrete Incorporating Coarse Aggregate*, in *Proceedings of Hipermat 2012 - 3rd International Symposium on UHPC and Nanotechnology for Construction Materials*. 2012, Kassel University Press: Kassel, Germany.
 38. Yang, S.L., et al., *Influence of aggregate and curing regime on the mechanical properties of ultra-high performance fibre reinforced concrete (UHPFRC)*. *Construction and Building Materials*, 2009. **23**(6): p. 2291-2298.
 39. B.P.Hughes and N.I. Fattuhi, *The Workability of steel-fibre reinforced concrete*. *Mag. Concr. Res.*, 1976. **28**: p. 157-161.
 40. ACI 544.3R-93, *Guide for specifying, proportioning, mixing, placing and finishing steel fibre reinforced concrete*. 1998.
 41. Kanstad, T. and e. al, *Forslag til retningslinjer for dimensjonering, utførelse og kontroll av fiberarmerte betongkonstruksjoner*, in *COIN Project report 29*. 2011, SINTEF Building and Infrastructure.
 42. Suter, R., et al., *Using UHPFRC for Complex Facade Elements*, in *Designing and building with UHPFRC - State of the Art and Development*, F. Toutlemonde and J. Resplendino, Editors. 2011, ISTE Ltd.: London. p. 405-419.
 43. Mazanec, O., D. Lowke, and P. Schiebl, *Mixing of high performance concrete: effect of concrete composition and mixing intensity on mixing time*. *Materials and Structures*, 2010. **43**(3): p. 357-365.
 44. Chang, P.-K. and Y.-N. Peng, *Influence of mixing techniques on properties of high performance concrete*. *Cement and Concrete Research*, 2001. **31**(1): p. 87-95.
 45. Simon, A., *NEW AFGC Recommendations on UHPFRC: Chapter 1 - Mechanical Characteristics and Behavior of UHPFRC*, in *Designing and building with UHPFRC - State of the Art and Development*, F. Toutlemonde and J. Resplendino, Editors. 2011, ISTE Ltd.: London. p. 723-741.
 46. Heinz, D., L. Urbonas, and T. Gerlicher, *Effect of Heat Treatment Method on the Properties of UHPC*, in *Proceedings of Hipermat 2012 - 3rd International Symposium on UHPC and Nanotechnology for Construction Materials*. 2012, Kassel University Press: Kassel, Germany.
 47. Ipek, M., et al., *Effect of pre-setting pressure applied to mechanical behaviours of reactive powder concrete during setting phase*. *Construction and Building Materials*, 2011. **25**(1): p. 61-68.
 48. İpek, M., K. Yilmaz, and M. Uysal, *The effect of pre-setting pressure applied flexural strength and fracture toughness of reactive powder concrete during the setting phase*. *Construction and Building Materials*, 2012. **26**(1): p. 459-465.
 49. Wille, K., A.E. Naaman, and G.J. Parra-Montesinos, *Ultra-High Performance Concrete with Compressive Strength Exceeding 150 MPa (22 ksi): A Simpler Way*. *ACI Materials Journal*, 2011(January-February).
 50. Berge, S., A. Rosenborg-Johnsen, and T.E.D. Dyrseth, *Developing High Performance Concrete with local materials*. 2012, University of Agder: Grimstad.
 51. Wang, C., et al., *Preparation of Ultra-High Performance Concrete with common technology and materials*. *Cement & Concrete Composites*, 2012. **34**(4): p. 538-544.
 52. Graybeal, B.A., *Material Property Characterization of Ultra-High Performance Concrete*. 2006, U.S Department of Transportation, Federal Highway Administration.
 53. Fehling, E., *Design relevant properties of hardened Ultra High Performance Concrete*, in *Proceedings of the international symposium on Ultra-High Performance Concrete - Heft 3*. 2011, University of Kassel, Germany: Kassel, Germany. p. 327-338.
 54. Graybeal, B.A., *Characterization of the behaviour of Ultra-High Performance Concrete*, in *Department of Civil and Environmental Engineering*. 2005, University of Maryland: College Park, MD, USA.

55. Aarup, B., *CRC: Precast Applications of UHPFRC*, in *Designing and building with UHPFRC - State of the Art and Development*, F. Toutlemonde and J. Resplendino, Editors. 2011, ISTE ltd.: London.
56. Resplendino, J., *Ultra High Performance Concrete: New AFGC Recommendations*, in *Designing and building with UHPFRC - State of the Art and Development*, F. Toutlemonde and J. Resplendino, Editors. 2011, ISTE ltd: London. p. 713-721.
57. Visage, E.T., et al., *Experimental and Analytical Analysis of the Flexural Behavior of UHPC Beams*, in *Proceedings of Hipermat 2012 - 3rd International Symposium on UHPC and Nanotechnology for Construction Materials*. 2012, Kassel University Press: Kassel, Germany.
58. Graybeal, B.A., et al., *Direct and Flexural Tension Test Methods for Determination of the Tensile Stress-Strain Response of UHPFRC*, in *Proceedings of Hipermat 2012 - 3rd International Symposium on UHPC and Nanotechnology for Construction Materials*. 2012, Kassel University Press: Kassel, Germany.
59. Hong, K.N., et al., *Material properties of air-cured ultra-high-performance steel-fiber-reinforced concrete at early ages*. International Journal of the Physical Sciences, 2010. **5**(17): p. 2622-2634.
60. Kang, S.T., et al., *The effect of fibre distribution characteristics on the flexural strength of steel fibre-reinforced ultra high strength concrete*. Construction and Building Materials, 2011. **25**(5): p. 2450-2457.
61. Kang, S.-T. and J.-K. Kim, *The relation between fiber orientation and tensile behavior in an Ultra High Performance Fiber Reinforced Cementitious Composites (UHPFRCC)*. Cement and Concrete Research, 2011. **41**(10): p. 1001-1014.
62. Kang, S.-T., et al., *Tensile fracture properties of an Ultra High Performance Fiber Reinforced Concrete (UHPFRC) with steel fiber*. Composite Structures, 2010. **92**(1): p. 61-71.
63. Zhang, W., Y. Zhang, and G. Zhang, *Single and multiple dynamic impacts behaviour of ultra-high performance cementitious composite*. Journal of Wuhan University of Technology--Materials Science Edition, 2011. **26**(6): p. 1227-1234.
64. Leonhardt, S., D. Lowke, and C. Gehlen, *Effect of Fibres on Impact Resistance of Ultra High Performance Concrete*, in *Proceedings of Hipermat 2012 - 3rd International Symposium on UHPC and Nanotechnology for Construction Materials*. 2012, Kassel University Press: Kassel, Germany.
65. Flietstra, J.C., et al., *Creep Behavior of UHPC under Compressive Loading with Varying Curing Regimes*, in *Proceedings of Hipermat 2012 - 3rd International Symposium on UHPC and Nanotechnology for Construction Materials*. 2012, Kassel University Press: Kassel, Germany.
66. Garas, V.Y., K.E. Curtis, and L.F. Kahn, *Creep of UHPC in tension and compression: Effect of thermal treatment*. Cement & Concrete Composites, 2012. **34**: p. 493-502.
67. Scheydt, J.C. and H.S. Mueller, *Microstructure of Ultra High Performance Concrete (UHPC) and its Impact on Durability*, in *Proceedings of Hipermat 2012 - 3rd International Symposium on UHPC and Nanotechnology for Construction Materials*. 2012, Kassel University Press: Kassel, Germany.
68. Toledo Filho, R.D., et al., *Performance assessment of Ultra High Performance Fiber Reinforced Cementitious Composites in view of sustainability*. Materials & Design, (0).
69. Pimienta, P., et al., *Literature Review on the Behaviour of UHPFRC at High Temperature*, in *Proceedings of Hipermat 2012 - 3rd International Symposium on UHPC and Nanotechnology for Construction Materials*. 2012, Kassel University Press: Kassel, Germany.
70. Way, R. and K. Wille, *Material Characterization of an Ultra High-Performance-Fibre Reinforced Concrete under Elevated Temperatures*, in *Proceedings of Hipermat 2012 - 3rd International Symposium on UHPC and Nanotechnology for Construction Materials*. 2012, Kassel University Press: Kassel, Germany

Appendix 1

AFGC-SETRA, Ultra-High Performance Fibre-Reinforced Concrete, interim recommendations: Compressive strength [4]

1.3. Résistance à la compression

Le comportement en compression est défini par la résistance caractéristique en compression et le module d'élasticité.

Pour les calculs réglementaires en flexion à l'ELU, on adopte une loi de comportement conventionnelle linéaire avec un palier plastique.

Le début du palier plastique correspond à une contrainte maximale égale à $0,85 f_{c28} / \theta^{\gamma_b}$.

Un exemple de courbe de comportement en compression est donné en annexe 1.

Essai :

L'éprouvette est un cylindre de $\varnothing 7 \times 14$ cm ou de $\varnothing 11 \times 22$ cm. L'essai de compression est piloté en force. La valeur caractéristique f_{ck} de la résistance à la compression est obtenue selon la même méthode que celle des bétons ordinaires telle que décrite dans le fascicule 65A. Un surfaçage lapidaire est indispensable pour effectuer les essais, et celui-ci doit faire l'objet d'un soin particulier.

1.3. Compressive strength

Compressive behaviour is defined by the characteristic compressive strength and the modulus of elasticity.

For the regulatory calculations regarding ULS bending, a conventional linear constitutive law with a yield plateau will be used.

The start of the yield plateau will correspond to a maximum stress of $0.85 f_{ck} / \theta^{\gamma_b}$.

An example of a compressive behaviour test curve is given in annex 1.

Test :

The test specimen shall be a $\varnothing 7 \times 14$ cm or $\varnothing 11 \times 22$ cm cylinder. The compressive-strength test load shall be force-controlled. The characteristic value f_{ck} of compressive strength shall be obtained using the same method as that used for ordinary concretes, as described in fascicule 65A (General Technical Specifications – Construction of Reinforced or Post-Tensioned Prestressed Concrete Civil Engineering Structures).



Interim recommendations 17

S'il est nécessaire de faire une étude non-linéaire de stabilité de forme, un pilotage en déplacement est nécessaire afin d'obtenir le comportement post-pic.

The surface must be carefully polished prior to testing.

If non-linear buckling calculations are needed, a displacement-controlled test shall be used in order to determine post-peak behaviour.

Appendix 2

AFGC-SETRA, Ultra-High Performance Fibre-Reinforced Concrete, interim recommendations: Tensile behaviour [4]

1.4. Comportement à la traction

1.4. Tensile behaviour

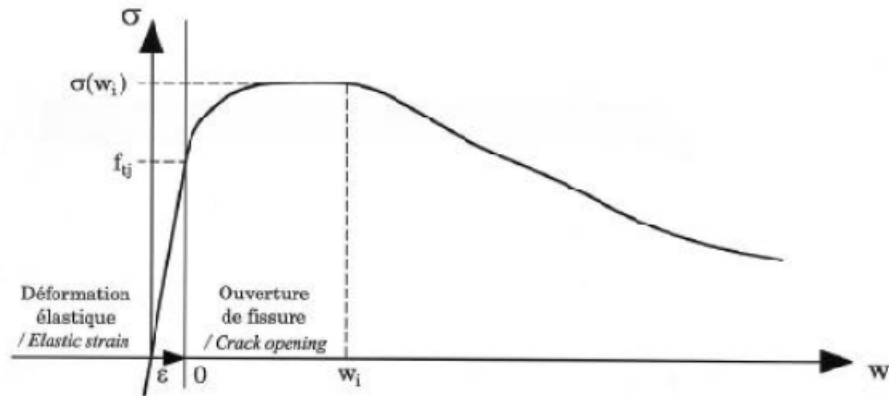


Figure 1.2: Exemple de loi de comportement en traction d'un BFUP (cas d'un matériau écouissant)

Figure 1.2: Example of tensile constitutive law of a UHPFRC (case of a strain-hardening material)

Le comportement en traction du matériau est caractérisé par :

- Un domaine de déformation élastique limitée par la résistance en traction de la matrice cimentaire f_{tj} ,
- Un domaine post-fissuration caractérisé par la résistance en traction du matériau fibré obtenue après fissuration de la matrice.

Si un temps de malaxage suffisant et des conditions de mise en œuvre assez traditionnelles permettent de garantir une faible dispersion de la résistance en traction de la matrice cimentaire f_t , la résistance en traction apportée par les fibres est en revanche très sensible aux conditions de réalisation :

The tensile behaviour of UHPFRC is characterized by:

- an elastic stage limited by the tensile strength of the cement matrix, f_{tj} ,
- a post-cracking stage characterized by the tensile strength of the composite material after the matrix has cracked.

Although sufficient mixing time and quite traditional placing conditions ensure low scatter of the tensile strength of the cement matrix, f_t , fibre tensile strength depends very much on the mixing and placement process:

18 - Recommandations provisoires

- Tout écoulement éventuel lors de la mise en œuvre tend à orienter les fibres dans le sens de l'écoulement,
 - Les fibres proches des parois sont naturellement orientées parallèlement aux coffrages. Ce phénomène n'intervient que sur une profondeur inférieure ou égale à la longueur des fibres. Il a ainsi d'autant plus d'influence sur la résistance en traction effective des pièces que l'épaisseur des structure est proche de la dimension des fibres.
 - Une orientation privilégiée des fibres dans le sens de la gravité peut parfois se produire, liée au comportement naturel des fibres dans la phase liquide visqueuse que constitue le béton avant la prise.
- *Any flow during concrete placing tends to align fibres in the direction of flow,*
 - *Fibres close to formwork walls are naturally aligned parallel to them. This phenomenon ceases beyond a distance from the formwork in excess of the fibre length. The closer component thicknesses are to the length of fibres, the greater is the effect on the effective tensile strength of the parts.*
 - *Preferential gravitational orientation of fibres can sometimes occur, due to the natural behaviour of fibres in the viscous-liquid phase of concrete before it sets.*

Les méthodes développées dans les présentes recommandations permettent d'intégrer l'ensemble de ces phénomènes qui sont dissociés en deux approches.

A partir d'essais de caractérisation qui dépendent du type de structure étudié (plaques minces, plaques épaisses, poutres ou coques), et qui peuvent être de deux types (traction directe ou traction par flexion), les recommandations donnent les coefficients permettant de passer des résultats des essais à une loi de comportement en traction « intrinsèque », à savoir qui ne dépend pas de la taille des éprouvettes et du type d'essai réalisé. Dans ce chapitre, et pour chaque protocole d'essais proposé, les recommandations donnent les coefficients correcteurs à appliquer pour aboutir aux lois de comportement intrinsèques.

Une fois la loi de comportement en traction intrinsèque déterminée, les recommandations donnent les éléments permettant d'intégrer l'influence des méthodes de mise en œuvre sur les valeurs de résistance réelle à prendre en compte dans les calculs. Cette correction à apporter aux courbes de résistances intrinsèques consiste à appliquer un coefficient correcteur $1/K$, qui est le coefficient de passage entre la loi intrinsèque et celle issue d'essais sur éprouvettes prélevées dans la structure réelle.

The methods outlined in these Recommendations take account of all these phenomena which are dissociated in two approaches.

Using characterization tests depending on the type of structure studied (thin slabs, thick slabs, beams, shells), and which can be of two types (direct tensile test or flexural tensile test), these Recommendations give the transfer factors to go from test results to an "intrinsic" curve for tensile behaviour which does not depend on test specimen size or on the type of test used. This chapter gives the corrective factors to be applied with each proposed test procedure to get intrinsic constitutive laws.

The Recommendations also give instructions for taking account of the effect placement methods have on the real strength values to be considered in calculations (once the intrinsic curve for tension has been determined). This correction of the intrinsic strength curves consists in applying a reduction coefficient $1/K$ representing the difference between the intrinsic curve and what would have been obtained on specimens taken from an actual structural element.



Pour déterminer ce coefficient K, plusieurs alternatives sont possibles :

- soit les méthodes de mise en œuvre prévues ont déjà été validées sur des ouvrages similaires réalisés de façon analogue à la structure projetée. Dans ce cas le projecteur utilise les coefficients de passage de la référence connue,
- soit il est prévu ultérieurement de justifier les méthodes de mises en œuvre sur la base d'épreuves de convenance réalisées sur un modèle représentatif de la structure réelle. Dans ce cas, le projecteur peut utiliser en première approche les valeurs de K obtenues sur des ouvrages similaires connus. Dans le chapitre 2 et dans les annexes du présent document, sont ainsi indiquées, à titre d'exemple, les valeurs et la méthodologie d'obtention du coefficient K dans le cas des ouvrages expérimentaux de Bourg-lès-Valence.

1.4.1 Résistance à la traction par traction directe

Protocole d'essai

Le protocole de réalisation de l'essai de traction directe est défini dans les Recommandations de l'A.F.R.E.M (référence [1.1]).

Sur la base de ces recommandations et à partir des résultats d'essais des chantiers de Chinon et Cattenom avec le BPR et le BSI il est apparu que le processus de traction directe sur éprouvette entaillée était très pénalisant et pas forcément représentatif du comportement du matériau dans la structure.

En effet le prélèvement est très local et de plus la taille du ligament du corps d'éprouvette est telle que la dispersion est grande.

There are two possible alternatives for determining this K factor:

- *Either the concrete placement methods have already been validated on similar works built in a manner similar to that proposed for the project, in which case the designer uses the K factors for the known reference,*
- *Or it is proposed to substantiate the placement methods at a later date, on the basis of suitability tests conducted on a representative model of the actual structure. In this case, the designer can approximate using the K values obtained on similar works. The K values obtained on the innovative Bourg-lès-Valence works, and the way they were obtained, are given as examples in Chapter 2 and in the annexes.*

1.4.1 Direct tensile strength

Test procedure

The direct tensile-strength test procedure is defined in the AFREM recommendations (reference [1.1]).

From these recommendations and the results of testing of BPR and BSI concretes at the Chinon and Cattenom nuclear power plants, it was seen that the direct tensile test using notched specimens is extremely unfavourable and not necessarily representative of the behaviour of the material in a structure.

This is because sampling is very localized, and because the size of the necked section induces broad scatter of results.

20 - Recommandations provisoires

Dans [1.3], vingt essais de traction directe ont été réalisés sur du Ductal®. Les éprouvettes sont des prismes 7*7*28 cm usinés en partie centrale (section centrale 7*5 cm).
 Les résultats obtenus étaient les suivants :

- Moyenne des résistances en traction directe (effort maximal divisé par la section): 10,27 MPa,
- Ecart type : 1,19 MPa,
- Valeur caractéristique réellement obtenue : 8.2 MPa

Valeur caractéristique de calcul : 8 MPa.

Les résultats de ces essais viennent corroborer les valeurs déduites des essais de flexion.

*In [1.3], twenty axial tensile-strength tests were carried out on Ductal®. The specimens were 7*7*28 cm prisms machined at the centre (central section measuring 7*5 cm).
 Results obtained:*

- *Mean direct tensile strength (maximum force divided by sectional area): 10.27 MPa*
- *Standard deviation: 1.19 MPa*
- *Characteristic value actually obtained: 8.2 MPa*

Design value : 8 MPa.

The results of these tests corroborate the values deduced from flexural tests.

1.4.2 Résistance à la traction par flexion

1.4.2 Flexural tensile strength

Protocole d'essai

Test procedure

Le protocole de réalisation de l'essai de traction par flexion est défini en annexe 2.

The flexural tensile-strength test procedure is given in annex 2.

Lors du chantier Cattenom, les essais de flexion de contrôle sur 196 éprouvettes 4*4*16 testées en flexion 3 points ont conduit aux résultats suivants :

- Résistance moyenne : 41,8 MPa
- Ecart type : 4,6 MPa
- Valeur caractéristique réellement obtenue : 33,9 Mpa
-

La résistance à la traction est déduite de cette valeur en utilisant une modélisation [1.3].

On obtient alors $f_t = 33,9 / 4,2 = 8,1$ Mpa

d'où la valeur caractéristique de 8 MPa pour f_t .

*Flexural tensile-strength checks carried out during the works at the Cattenom nuclear power plant on 196 specimens measuring 4*4*16 cm tested on a centre-point bending press gave the following results:*

- *Mean strength: 41.8 MPa*
- *Standard deviation: 4.6 MPa*
- *Characteristic value actually obtained: 33.9 MPa*

The tensile strength is deduced from this value by means of modelling [1.3].

This gives $f_t = 33.9 / 4.2 = 8.1$ MPa

whence the design value of 8 MPa for f_t .

1.4.3 Plaques minces

Corps d'épreuve

Les plaques minces sont des éléments dont l'épaisseur e est telle que :

$$e \leq 3 L_f \quad \text{avec } L_f = \text{longueur de la fibre}$$

et

$$\frac{L}{e} \geq 50 \quad \text{avec } L = \text{portée de la structure}$$

Pour ce genre de plaque, le mode caractéristique de travail étant la flexion, le comportement en traction est caractérisé par un essai de flexion 4 points sur des bandes prismatiques rectangulaires d'épaisseur égale à celle de la structure, de longueur 20 fois l'épaisseur e et de largeur au moins égale à $8 L_f$.

1.4.3 Thin slabs

Specimen

Thin slabs are elements whose thickness e is such that :

$$e \leq 3 L_f \quad \text{where } L_f = \text{length of individual fibres}$$

and

$$\frac{L}{e} \geq 50 \quad \text{where } L = \text{span of slab}$$

Since this kind of slab characteristically works in bending, the tensile strength is characterized by a third-point flexural test using rectangular prismatic specimens. The specimens are the same thickness as the structure; their length is 20 times thickness e , and their width is greater than $8 L_f$.

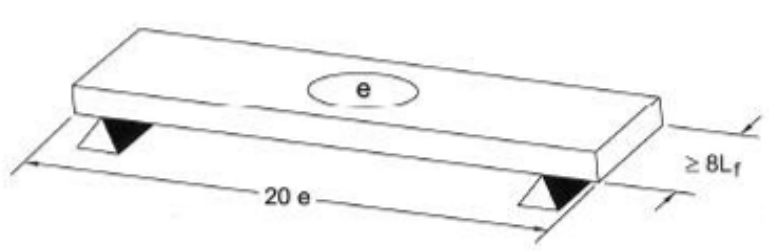


Figure 1.3 : Plaques minces : définition du prisme d'essai
Figure 1.3 : Thin slabs : definition of the test prism

Protocole d'essai

L'essai de flexion est piloté en déplacement. Le résultat de l'essai (courbe effort – flèche au centre) est analysé de manière inverse avec une loi de comportement de type contrainte – déformation, car on peut considérer que pour ce type de structure, de sollicitation et de matériau, une multi-fissuration diffuse sera obtenue.

La minceur des plaques et leur mode de coulage sont susceptibles d'influencer l'orientation des fibres. On peut donc s'attendre à des performances post-fissuration qui varient selon la direction considérée d'une plaque. Les essais doivent mettre en évidence cette éventuelle anisotropie.

Test procedure

The flexural tensile-strength test is displacement-controlled. The result of the test (force–mid-span deflection curve) is back-analyzed using a stress-strain type constitutive law since it can be considered that for this kind of structure, loading, and material, diffuse multiple cracking will occur.

The thinness of the slabs and the way the concrete is placed are likely to affect the orientation of fibres. It can therefore be expected that post-cracking performance will vary, depending on the direction tested. Testing must reveal any such anisotropy.

22 - Recommandations provisoires

Le détail du protocole d'essai recommandé est donné en annexe 3.

L'objectif principal de la démarche est de n'avoir besoin, à terme, que des résultats d'essais sur bandes pour justifier les performances de structures de type plaques minces.

Si l'on a besoin de caractéristiques du comportement au poinçonnement il est recommandé d'utiliser l'un des essais suivants :

- l'essai AFTES (pour béton projeté) ou essai SNCF.
- l'essai de flexion sous charge ponctuelle centrée d'une dalle circulaire [1.17]
- l'essai pour plaques de faux planchers (4 appuis ponctuels) – Norme NF P 67-101

1.4.4 Plaques épaisses

Corps d'épreuve

Les plaques épaisses sont des éléments dont l'épaisseur e est telle que :

$$e > 3 L_f \quad \text{où } L_f = \text{longueur de la fibre}$$

et

$$\frac{L}{e} \geq 10 \quad \text{où } L = \text{portée de la dalle}$$

Trois types d'essais sont envisageables :

- Essais de flexion 3 points sur prisme entaillé piloté en déplacement avec une mesure de la flèche au centre et analyse inverse pour obtenir une courbe contrainte – ouverture de fissure en traction. Cet essai est considéré comme pénalisant.
- Essais de traction directe sur des éprouvettes entaillées prismatiques sciées ou cylindriques carottées dans des prismes.
-
-

The recommended test procedure is described in annex 3.

The main objective of the procedure is to eventually need only test results on strips to check the performance of thin-slab type structures.

If the characteristics of punching behaviour are required, it is recommended to use one of the following tests:

- *the French Tunnelling Association (AFTES) test or the French Rail (SNCF) test, both for sprayed concrete.*
- *the flexural test with a point load centred on a circular slab [1.17]*
- *the raised-flooring test (4 point bearings) – French standard NFP 67-101*

1.4.4 Thick slabs

Specimen

Thick slabs are elements whose thickness e is such that:

$$e > 3 L_f \quad \text{where } L_f = \text{length of individual fibres}$$

and

$$\frac{L}{e} \geq 10 \quad \text{where } L = \text{span of slab}$$

Three types of test may be used:

- *Centre-point flexural test using notched prisms (displacement controlled), with measurement of mid-span deflection and back analysis to derive a "stress - crack opening under tension" curve. This test is deemed to give unfavourable results.*
- *Direct tensile-strength test on notched sawn prismatic specimens or cylindrical specimens cored from prisms.*



- Essais de traction directe sur éprouvettes non entaillées. Cet essai ne permet d'obtenir une information fiable que pour de très faibles ouvertures de fissures.

Six éprouvettes au minimum doivent être testées. Les dimensions des prismes proposés sont fonction de la taille des fibres :

- $L_f \leq 15$ mm : 7 x 7 x 28 cm,
- $15 < L_f \leq 20$ mm : 10 x 10 x 40 cm,
- $20 < L_f \leq 25$ mm : 14 x 14 x 56 cm,
- $25 < L_f$: largeur $> 5 L_f$, hauteur $> 5 L_f$ ou égale à l'épaisseur de la structure si celle-ci est connue, longueur = 4 fois la hauteur.

Protocole d'essai par flexion 3 points

Les éprouvettes sont testées face coffrée en bas. Les éprouvettes utilisées pour les essais de traction sont prélevées de manière à ce que la direction de traction directe soit parallèle à l'axe longitudinal du prisme.

Le prisme est coulé depuis une seule extrémité afin de garantir une répétabilité de réalisation. Les moules sont vibrés sur une table et arasés à la règle vibrante.

Le détail du protocole d'essai et son exploitation sont donnés en annexe 2.

1.4.5 Poutres

Les cas de charge à considérer pour calculer une poutre sont très nombreux :

- flexion longitudinale,
- flexion transversale,
- effort tranchant,
- torsion,
- diffusion de la précontrainte,
- efforts localisés.

- *Direct tensile-strength tests on un-notched specimens. This test produces reliable information only for very small crack widths.*

Test at least six specimens. The dimensions of the test prisms proposed depend on the size of fibres:

- $L_f \leq 15$ mm : 7 x 7 x 28 cm,
- $15 < L_f \leq 20$ mm : 10 x 10 x 40 cm,
- $20 < L_f \leq 25$ mm : 14 x 14 x 56 cm,
- $25 < L_f$: width $> 5 L_f$, height $> 5 L_f$ or equal to the thickness of the structure, if known, length = 4 times the height.

Centre-point flexural test procedure

Test the specimens with the moulded face downwards. Take the specimens used for tensile-strength tests such that the direction of axial tension is parallel to the longitudinal axis of the prism.

Cast the prism from one end only to ensure good casting repeatability. Vibrate the moulds on a table and level the concrete with a vibrating striker.

A description of the test procedure and its interpretation method are given in annex 2.

1.4.5 Beams

There are many load cases to be considered for designing beams:

- *longitudinal bending*
- *transverse bending*
- *shear strength*
- *torsion*
- *distribution of prestress*
- *localized forces.*

24 - Recommandations provisoires

La démarche de caractérisation adoptée est ainsi la suivante :

Réalisation d'un essai de flexion sur prisme coulé entaillé à partir duquel une analyse inverse conduit à une loi de traction post-fissuration contrainte – ouverture de fissure ($\sigma - w$).

La loi issue de cet essai est corrigée pour intégrer les effets d'échelles et de parois, liés à la géométrie et au mode de confection des éprouvettes.

La loi de comportement obtenue est ensuite pondérée par un coefficient réducteur $1/K$ représentant l'écart entre la loi issue d'essais sur prisme coulé et celle qu'on obtient en prélevant des prismes dans l'élément de structure fabriqué.

Afin de déterminer un coefficient de passage K exact pour l'application particulière considérée, il est nécessaire de réaliser des éléments de géométrie et de mode de fabrication représentatifs de la structure réelle, puis de prélever des éprouvettes dans les directions des contraintes principales.

Les dimensions des prismes sont celles proposées pour le cas des dalles épaisses si la géométrie de la poutre n'est pas connue a priori. Dans le cas contraire on pourra choisir comme largeur et hauteur des prismes deux fois le rayon moyen de la poutre.

Les prismes sont coulés de manière à limiter au maximum une orientation préférentielle des fibres. Après remplissage, ils sont vibrés si nécessaire.

Les prismes sont testés en flexion en les ayant tourné d'un quart de tour par rapport au sens de coulage afin de limiter les effets de la paroi inférieure.

Résistance en traction f_{tj}

Cette résistance est obtenue à partir d'essais de flexion 4 points sur prismes non entaillés (dimensions définies en annexe 2). La résistance est déterminée par la perte de linéarité du comportement initial, relevée sur les courbes effort en fonction de la flèche.

The characterization procedure adopted is as described below.

Cast and notch a prism. Perform a flexural test with it. Conduct back analysis to determine a post-cracking stress-crack width ($\sigma - w$) law.

Correct the law derived from this test so as to integrate scale and face effects associated with the specimen shape and casting method.

Weight this law with a reduction coefficient $1/K$ representing the difference between a flexural test result for a cast prism and what would have been obtained on prisms sawn from an actual structural element.

To determine an exact transfer factor K for the particular application considered, make components that are representative of the actual geometry and manufacturing method used for the structure, and take specimens along the directions of principal stress.

The dimensions of the prisms are those proposed for thick slabs if the shape of the beam is not known. Otherwise, the width and height of the prism can be twice the mean radius of the beam.

Cast prisms so as to limit preferential orientation of fibres as much as possible. After filling, vibrate the prisms if necessary.

For flexural-strength testing, turn the prisms 90° from the casting position in order to limit the effects of the underside.

Tensile strength f_{tj}

Tensile strength f_{tj} is given by third-point flexural tests on un-notched prisms (dimensions defined in annex 2). It is the strength read at the end of the initial linear behaviour on force-deflection curves.

Le détail du protocole d'essai est donné en annexe 2.

Test procedure details are given in annex 2.

Loi de comportement post-fissuration

Cette partie de la loi de comportement en traction, est déterminée par des essais de flexion 3 points sur prismes entaillés. Ces essais correspondent au protocole défini dans l'annexe 2.

Post-cracking constitutive law

This part of the tensile constitutive law is given by centre-point flexural tests on notched prisms. The procedure for these tests is given in annex 2.

L'entaille, pratiquée en section centrale sur une hauteur équivalente à 10% de la hauteur du prisme, localise la fissure.

The notch is made at mid-span, to a depth of 10% of the total prism height, to induce cracking at a known location.

Au minimum 6 essais sont réalisés et analysés en termes de moyenne et de courbe caractéristique.

Carry out at least 6 tests and analyze their results (mean value and characteristic curve).

La loi caractéristique contrainte – ouverture de fissure ($\sigma - w$) peut être obtenue soit par analyse inverse ([1.11], [1.12], [1.13]) décrite en annexe 2, soit par calculs itératifs avec la méthode directe de flexion en section fissurée en cherchant à égaler les surfaces sous les courbes moment-ouverture de fissure.

The characteristic stress-crack width ($\sigma-w$) law can be derived either by back analysis ([1.11], [1.12], [1.13]) as described in annex 2, or by iterative calculation with the direct tensile-strength method for cracked sections, aiming to make the areas below the bending moment-crack width curves the same.

La loi caractéristique obtenue est exploitée de manière à déterminer une loi en traction simplifiée (linéarisée) munie de valeurs caractéristiques telle que proposée ci-dessous :

The characteristic law obtained is used to determine a simplified (linearized) tensile-strength law such as that proposed below:

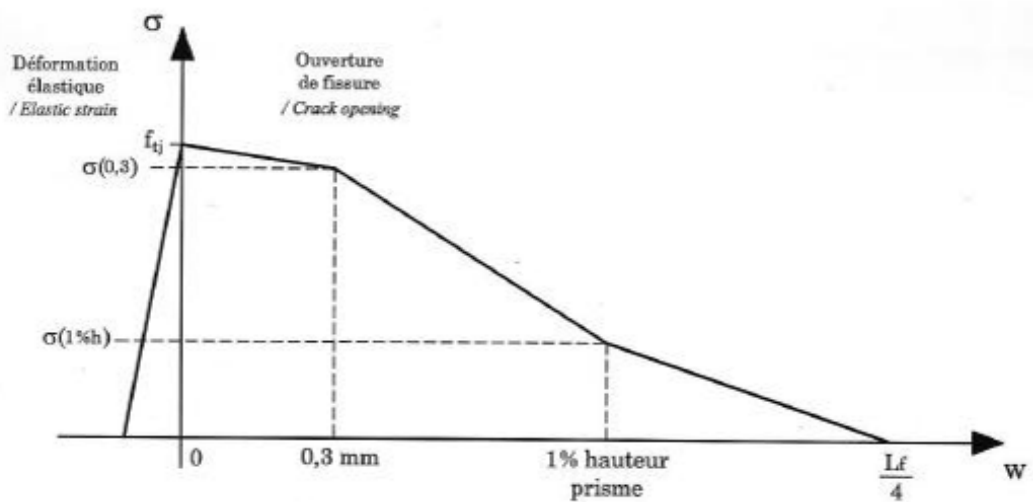


Figure 1.4 : Loi simplifiée en traction

Figure 1.4 : Simplified tensile-strength law

26 - Recommandations provisoires

1.4.6 Coques

Les coques ne sont pas considérées comme un type particulier de structures :

- Les coques épaisses sont traitées comme des poutres : les éprouvettes sont alors des prismes,
- Les coques minces sont traitées comme des dalles minces.

1.4.7 Récapitulatif

L'ensemble des essais de caractérisation qui viennent d'être évoqués peut être résumé de la façon suivante :

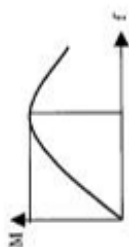
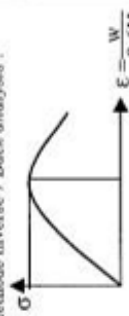
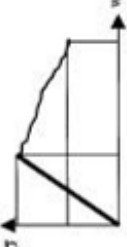
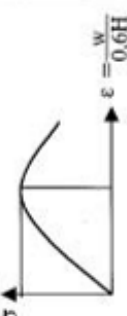
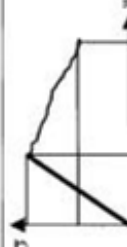
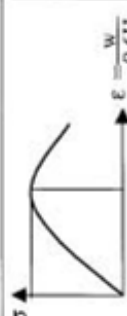
1.4.6 Shells

Shells are not considered to be a separate kind of structural element:

- *thick shells are designed in the same way as beams: the test specimens are prisms*
- *thin shells are designed in the same way as thin slabs*

1.4.7 Summary

All the characterization tests described above are summed up overleaf:

Type de Structure / Type of structure	Essais / Tests	Résultats d'essais / Test result	Résultats exploitables / Usable result Méthode inverse / Back analysis :
PLAQUES MINCES / THIN SLABS	Essai de flexion 4 points sur éléments représentant l'élément réel. / Third-point flexural tests on specimens representing actual elements		
	Essai de flexion 3 points sur éprouvette entaillée. / Centre-point test on notched specimens		
POUTRES / BEAMS	Ou essai de traction directe sur éprouvette entaillée. / Or direct tensile-strength test on notched specimens		
	Ou essai de traction sur éprouvette non entaillée / Or direct tensile-strength test on un-notched specimens		
	Essai de flexion 3 points sur éprouvette entaillée. / Centre-point test on notched specimens		
	Ou essai de traction directe sur éprouvette entaillée. / Or direct tensile-strength test on notched specimens		

Appendix 3

AFGC-SETRA, Ultra-High Performance Fibre-Reinforced Concrete, interim recommendations: Annex 2 – Experimental Procedure for flexural tensile tests on prisms and analysis method [4]



Interim recommendations 103

ANNEXE 2

Protocole expérimental des essais de flexion sur prismes et méthode d'exploitation

Introduction

Cette annexe décrit les procédures expérimentales pouvant être mises en œuvre afin de caractériser les performances en traction des BFUP par le biais d'essais de flexion. Deux types d'essais sont proposés. D'une part des essais de flexion quatre points permettant d'accéder à la résistance en traction suite à une correction de l'effet d'échelle. D'autre part, des essais de flexion trois points sur prismes entaillés qui permettent d'accéder à la contribution des fibres comme renfort d'une section fissurée après application d'une méthode d'exploitation dite méthode inverse.

1. Dimensions des éprouvettes

Les éprouvettes sont des prismes de section carrée, de côté a et de longueur $4*a$, soit :

$a = 7 \text{ cm}$: prisme $7*7*28$
 $a = 10 \text{ cm}$: prisme $10*10*40$
 $a = 14 \text{ cm}$: prisme $14*14*56$
 $a = 20 \text{ cm}$: prisme $20*20*80$

Le choix de la dimension des éprouvettes est conditionné par la dimension des fibres et le type d'élément de structure à caractériser. Ces informations sont données directement au 1.4.4.

2. Préparation des éprouvettes

La préparation des éprouvettes (mode de coulage) ainsi que le mode d'essais (rotation des éprouvettes d'un quart de tour ou non) sont précisés dans le texte des recommandations en fonction du type de structure envisagé.

ANNEX 2

Experimental procedure for flexural tensile tests on prisms and analysis method

Introduction

This annex describes the experimental procedures that can be used to characterize the tensile performance of UHPFRC by means of flexural tests. Two types of test are proposed: firstly, third-point flexural tests for determining the tensile strength following correction for scale effect; secondly, centre-point flexural tests using notched prisms, to determine the contribution of fibres as reinforcement of a cracked section, after application of the so-called 'back-analysis' method.

1. Dimensions of test specimens

*The test specimens are square-section prisms of dimensions a by $4*a$ long:*

*$a = 7 \text{ cm}$: prism $7*7*28$
 $a = 10 \text{ cm}$: prism $10*10*40$
 $a = 14 \text{ cm}$: prism $14*14*56$
 $a = 20 \text{ cm}$: prism $20*20*80$*

The choice of specimen size is determined by the dimension of the fibres and the type of structural element to be characterized. The relevant information is given in §1.4.4.

2. Preparation of test specimens

The preparation of specimens (casting method) and the test method (whether specimens are turned 90° or not) are specified in the body of the Recommendations, in accordance with the type of structure envisaged.

104 - Recommandations provisoires

En accord avec les recommandations en cours de publication de la RILEM sur le dimensionnement de structure en Béton Renforcé de Fibres (groupe TC 162-TDF), pour les prismes entaillés, une entaille est sciée en section centrale, du côté de la face tendue lors de l'essai de flexion. La profondeur de l'entaille est égale à 10% de la hauteur du prisme, afin de permettre une localisation efficace de la fissure en minimisant les risques d'une fissuration hors entaille. La largeur de l'entaille doit être de l'ordre de 2mm.

3. Principe de l'essai

Les éprouvettes sont testées en flexion, trois points (flexion centrée) pour les prismes entaillés, quatre points (flexion circulaire) pour les prismes non entaillés. La longueur entre appuis inférieurs est égale à trois fois la hauteur du prisme. Ce principe est, là encore, conforme aux propositions du groupe RILEM TC 162-TDF.

4. Matériel utilisé

La machine d'essai est une presse de traction/compression de préférence servo-hydraulique pouvant être asservie en déplacement vérin ou de préférence sur un capteur externe.

Dans le cas des essais de flexion quatre point, un capteur de type LVDT doit être fixé par un dispositif spécifique sur l'échantillon afin de mesurer la flèche vraie de l'échantillon au cours de l'essai (figure 1). En effet, sans un tel dispositif, la mesure de la flèche est faussée par les tassements aux points d'application des forces et aux appuis ainsi que par les déformations du montage lui-même.

Dans le cas des essais de flexion trois points, un capteur pontant l'entaille est fixé sur le prisme. Ce capteur doit être fixé au niveau de la fibre tendue inférieure du prisme. Il peut s'agir d'un capteur type LVDT ou d'un capteur spécifique de type extensométrique. Ce capteur est fixé par l'intermédiaire de plots collés de part et d'autre de l'entaille. La colle est une colle rapide type cyano-acrylate.

In accordance with the RILEM recommendations on the design of Fibre-Reinforced Concrete structures (TC 162-TDF) currently at press, notched prisms are to be sawn at the centre, on the side under tension during the flexural test. The depth of the notch is 10% of the prism height, in order to effectively determine the location of cracking and minimize the risk of cracking beyond the notch area. The notch should be about 2 mm wide.

3. Principle of test

Bend-test notched specimens with a centre-point machine (angular bending) and un-notched specimens with a third-point machine (circular bending). The distance between bearing points must be three times the depth of the prism; this is in accordance with the recommendations of RILEM TC 162-TDF.

4. Equipment used

The test machine is a tensile/compressive load frame, preferably hydraulic and controlled by jack displacement or, even better, with an external sensor.

In the case of third-point bending, an LVDT type sensor must be attached to the specimen by special means in order to measure the actual deflection of the specimen during testing (Figure 1). Without such a system, deflection measurement is contaminated by settlement at the loading points and bearings and by deformation of the test apparatus itself.

For centre-point bending, fix a sensor to the prism, bridging the notch. Attach it to the tensile bottom fibre. It can be an LVDT type sensor or a special type of extensometric sensor. Attach it by means of tabs glued on each side of the notch. Use a fast-setting cyano-acrylate type glue. The distance between tabs must be constant from one test to the next so that the initial measurements can be corrected by subtracting the elastic deformation.

La distance entre les plots doit être constante d'un essai à l'autre afin de corriger les mesures initiales par soustraction de la déformation élastique. Cette distance est de l'ordre de 4 à 5 cm. Il demeure possible en fonction du type de machine d'essais utilisée de compléter l'instrumentation des prismes entaillés par un capteur de mesure de la flèche comme dans le cas des essais de flexion quatre points.

The distance between tabs should be around 4 to 5 cm. Depending on the type of test machine, it may also be possible to complement the instrumentation of the notched specimens with a deflection measuring sensor, as for the third-point flexural tests.

La course des capteurs doit être d'au moins 2 mm avec une précision de 0.5% pleine échelle.

The stroke of the sensors must be at least 2 mm, with accuracy to within 5% at full scale.

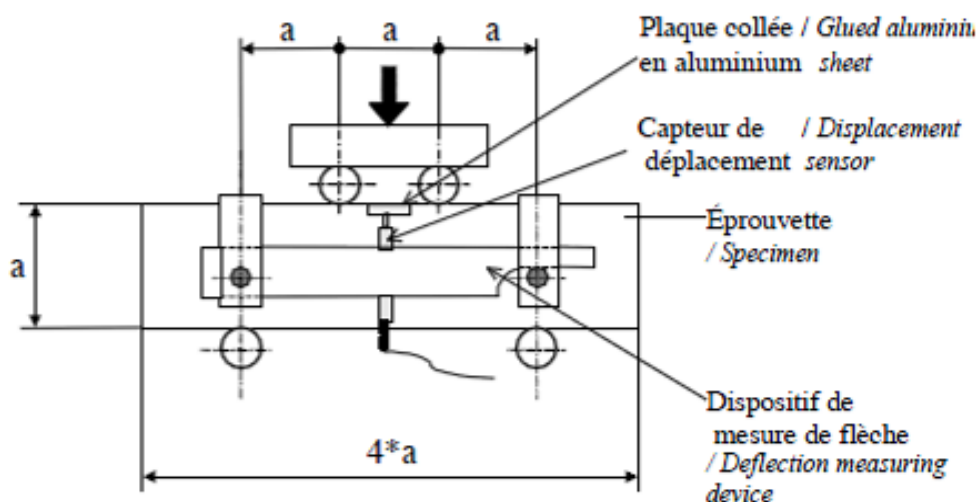


Figure 1 : Principe de mesure de la flèche vraie dans le cas d'un essai de flexion quatre points

Figure 1: Principle for measuring actual deflection with third-point flexural test

5. Mode opératoire

L'éprouvette est mise en place sur le dispositif d'essai de flexion de la presse. Les capteurs sont fixés sur l'éprouvette.

Une précharge est alors appliquée sur l'éprouvette, d'intensité aussi faible que possible, de l'ordre de quelques kilo-newtons, qui doit être prise en compte dans la suite de l'essai. Il faut s'assurer que lors de l'application de cette précharge, les capteurs de flèche et de mesure de l'ouverture de fissure répondent.

5. Test procedure

Place the specimen on the bending test device in the press. Fix the sensors to the specimen.

Preload the specimen to as small a degree as possible (around a few kN). This load is to be taken into account in the subsequent test procedure. Check that when this preload is applied, the deflection sensors and the sensors for measuring crack width respond.

106 - Recommandations provisoires

L'application de cette précharge peut être effectuée de différentes manières :

- par contrôle en déplacement piston (en commande manuelle et automatique), dans le cas où le système de commande de la presse permet de détecter une limite en force et de la maintenir,
- par contrôle en force : dans ce cas une approche très précise en déplacement manuel du vérin doit permettre de limiter la distance entre l'éprouvette et les points d'application de la charge à environ 1 millimètre. La boucle ouverte créée lors du passage en contrôle de force ne dure pas longtemps et il suffit de détecter la valeur de la précharge dès que le contact est établi (boucle d'asservissement fermée) et la valeur requise atteinte,

Basculer alors l'asservissement soit sur le capteur d'ouverture de fissure, soit sur le capteur de flèche (en mode automatique, après détection de la précharge, certaines presses poursuivent directement l'essai en basculant l'asservissement sur le capteur choisi).

Il est préférable, dans la mesure du possible, d'asservir l'essai directement sur un capteur fixé sur l'éprouvette (ouverture de fissure ou flèche). Cependant, dans le cas des presses qui ne supportent pas un asservissement sur un capteur externe, il demeure possible de piloter l'essai sur le déplacement du vérin. Les risques d'instabilité sont plus grands lors de la fissuration mais l'enregistrement de la flèche et de l'ouverture de la fissure sont exploitables.

Selon le capteur retenu pour le pilotage de l'essai, la vitesse de chargement doit être adaptée afin d'obtenir une bonne description du comportement tout en restant dans des limites raisonnables pour la durée de l'essai.

A titre d'ordre de grandeur, en pilotage vérin, une vitesse de l'ordre de 0,25 mm/mn convient, en pilotage sur la flèche, la vitesse est de 0,1 mm/mn et en pilotage sur le capteur pontant la fissure, elle est de l'ordre de 0,025 mm/mn. L'essai est poursuivi jusqu'à une flèche mesurée directement sur l'échantillon de $0,015^*a$ en mm, ce qui permet d'obtenir une durée d'essai raisonnable.

The preload can be applied in different ways:

- *by piston-displacement control (manually or automatically) if the press control system can detect a force limit and maintain it,*
- *by force control: in this case very precise manual control of the jack must limit the distance between the specimen and the loading points to about 1 millimetre. The transient when changing to force control does not last long, and it suffices to detect the value of preloading as soon as contact is made (control loop closed) and the required value is reached.*

Then switch control of loading to the crack sensor, or to the deflection sensor (in automatic mode, after detection of the preload, some presses continue the test immediately by switching control to the selected sensor).

In so far as possible, it is preferable to control the test directly from a sensor attached to the specimen (crack width or deflection). However, in the case of presses which do not allow for control from an external sensor, it is possible to control the test by jack displacement. The risks of instability are greater when cracking occurs, but the recorded deflection and crack width can be used nonetheless.

*Depending on the type of sensor chosen for controlling the test, the loading rate must be adapted to obtain a good description of the behaviour while remaining consistent with reasonable test durations. For guidance, with jack control a pace rate of about 0.25 mm/min. is suitable; with deflection control, the pace rate is 0.1 mm/min.; and with control from a sensor bridging the crack, it is about 0.025 mm/min. The test continues until the deflection measured directly on the specimen reaches 0.015^*a (in mm), which amounts to a reasonable test duration. The following table gives the deflection to be attained (when the test can be stopped) for different specimen sizes.*

Ainsi, en fonction de la taille des prismes, le tableau suivant donne la flèche à atteindre pour interrompre l'essai :

Prisme <i>Prism</i> (mm)	Flèche maximale <i>Maximum deflection</i> (mm)	Nombre de données <i>Amount of data</i> (fréquence 5Hz)
70*70*280	2	1200
100*100*400	2.5	1800
140*140*560	3	2520
200*200*800	3.5	3600

6. Acquisition des données

L'enregistrement des données au cours de l'essai doit être effectué avec une fréquence de 5 hertz, afin d'obtenir une courbe complète comportant un minimum de 1200 points. Dans le cas des échantillons de grandes dimensions, il est possible de réduire la fréquence d'acquisition tout en conservant un nombre de données suffisantes. Les signaux à enregistrer sont :

- le temps,
- l'ouverture de la fissure,
- la flèche,
- la force,
- éventuellement le déplacement du piston.

7. Mise en forme des résultats

Un minimum de six essais est requis afin d'obtenir une réponse moyenne statistiquement significative. La mise en forme des résultats s'effectue de la façon suivante :

7.1. Estimation de la résistance en traction, flexion 4 points, prismes non entaillés

A défaut d'essais de traction directe pour évaluer les performances du matériau, il est possible d'approcher cette caractéristique sur la base des essais de flexion 4 points. Il suffit d'extraire des essais de flexion la valeur de l'effort (F_{fiss}) correspondant à la perte de linéarité du comportement élastique. Ce point est aisément identifiable sur les courbes effort en fonction de la flèche vraie. Par suite, la résistance obtenue à la fissuration en flexion peut être calculée par la formule suivante :

6. Data acquisition

During the test, record data at a frequency of 5 hertz in order to provide a full curve with at least 1200 points. In the case of large specimens, the frequency of acquisition can be reduced yet still give enough data. The signals to be recorded are:

- *time,*
- *crack width,*
- *deflection,*
- *force,*
- *ram displacement (possibly).*

7. Conflation of results

At least six tests are required to get a statistically significant mean response. Results are conflated as follows:

7.1. Assessment of tensile strength, third-point bending, un-notched specimens

In the absence of direct tensile-strength testing to determine the performance of UHPFRC, the tensile strength can be approximated from third-point flexural testing by extracting from the flexural test results the value of the force (F_{fiss}) corresponding to the loss of linearity of elastic behaviour. This point is easily identified on force/actual-deflection curves. The strength (R_{fl}) attained at the moment of flexural cracking can then be easily calculated using the following formula:

108 - Recommandations provisoires

$$R_d = 3 \cdot F_{fss} / a^2$$

avec F_{fss} en N et a en mm, R_d est en MPa

Pour obtenir une estimation de la résistance en traction, il faut corriger cette résistance à la fissuration de l'effet d'échelle (ou effet de gradient). L'approche retenue est issue des travaux de recherche sur cet aspect et correspond à celle retenue dans le cadre du code de calculs des structures CEB-FIP, soit :

$$R_t = R_{ft} \cdot \frac{2.0 \cdot \left(\frac{h}{h_0}\right)^{0.7}}{1 + 2.0 \cdot \left(\frac{h}{h_0}\right)^{0.7}} \quad \text{avec } h_0 = 100 \text{ mm}$$

Pour appliquer une telle formule, il faut adopter pour h , la hauteur du prisme, soit a en mm.

7.2. Correction de l'ouverture de la fissure, flexion 3 points, prismes entaillés

Pour tenir compte de la déformation élastique sur la base de mesure, il est nécessaire de corriger la mesure directe de l'ouverture de fissure. Cette correction peut être effectuée uniquement avant localisation de la fissure, après, la décharge créée par la propagation de la fissure conduit à une déformation élastique négligeable sur la base de mesure.

La méthode la plus simple pour effectuer cette correction consiste à repérer la fin du domaine élastique initial (perte de linéarité) et de noter les valeurs de flèche (f_0) et d'ouverture de fissure correspondante (w_0). L'ouverture de fissure qui nous intéresse s'obtient alors directement en soustrayant la valeur w_0 aux valeurs mesurées de l'ouverture de fissure. Cette opération effectuée simplement un changement de repère et place la nouvelle origine de nos courbes à l'instant supposé de la localisation de la fissure.

Remarque : La déformation élastique sur la base de mesure de 50 mm est estimée à environ 10 μm . Cette valeur donne l'ordre de grandeur de la valeur w_0 qui doit être obtenue. Par ailleurs, cette valeur demeurant très faible,

$$R_{ft} = 3 \cdot F_{fss} / a^2$$

where F_{fss} is in newtons, a in millimeters, and R_{ft} in megapascals.

To estimate the tensile strength, the cracking strength must be corrected for scale effects (or gradient effect). The approach adopted is derived from research into this point and corresponds to that adopted for the CEB-FIP structural design code:

To apply such a formula, take as h the depth of the prism, i.e. a in millimetres.

7.2. Correction for crack width, centre-point bending, notched specimens

To take account of elastic deformation of the measurement base, it is necessary to correct the direct measurement of crack width. This correction can be carried out only before initiation of the crack; subsequently, the stress release caused by propagation of the crack results in negligible elastic deformation of the measuring base.

The simplest way to make this correction is to identify the end of the initial elastic range (loss of linearity) and to note the deflection values (f_0) and corresponding crack widths (w_0). The crack width of interest is then obtained directly by subtracting w_0 from the values measured when cracking started. This simply changes the co-ordinate system and puts the new origin of the curves at the time the crack is assumed to initiate.

Remark: The elastic deformation on a 50 mm measurement base is estimated to be about 10 μm . This gives the order of magnitude of the value w_0 to be obtained. Moreover, because this value remains very low, it is valid to simply move the origin to redefine the crack



L'hypothèse d'un simple changement d'origine pour définir l'axe des ouvertures de fissure est valide, les déformations élastiques résiduelles sur la base de mesure devenant très rapidement négligeables.

7.3. Corrélation entre l'ouverture de la fissure et la flèche, flexion 3 points, prismes entaillés

Dans le cas d'un essai où l'ouverture de la fissure n'est pas enregistrée, il faut l'estimer à partir de la mesure de la flèche vraie. Bien que cette relation ne soit pas directe et dépende de la hauteur de la fissure, une bonne estimation peut être obtenue de la façon suivante.

Connaissant la flèche f_0 qui correspond à la fin du domaine élastique (voir paragraphe 7.2), l'ouverture de la fissure (w) est alors estimée par la relation suivante :

$$w = 4/3 * 0.9 * (f - f_0)$$

où f représente la flèche vraie mesurée.

Cette expression est issue de l'hypothèse d'un mécanisme de rotule parfaite au droit de la fissure, affectée d'un coefficient correcteur qui prend en compte le fait que la fissure ne traverse pas totalement la section. Elle n'est donc pas valide en période initiale de propagation de la fissure. Cependant, cette période est relativement courte et la hauteur de la fissure se stabilise rapidement entre 80 et 90% de la hauteur de la section.

Remarque : cette approche ne doit être mise en œuvre qu'en tout dernière issue compte tenu de la diversité des réponses d'un matériau à l'autre.

7.4. Filtrage des données, flexion 3 points, prismes entaillés

Cette opération a pour but de réduire le bruit des données expérimentales afin de faciliter la mise en œuvre de la méthode inverse. Il va de soi que plus la qualité des essais est bonne, plus cette opération de filtrage est aisée. Dans tous les cas, lorsqu'un résultat d'essais présente des sauts brusques, soit en effort, soit en déplacement (flèche ou ouverture de fissure), qui correspondent manifestement à des problèmes d'accroissement lors de l'essai, aucun

simple move the origin to redefine the crack-width scale, since the residual elastic deformation of the measuring base very quickly becomes negligible.

7.3. Correlation between crack width and deflection, centre-point, notched specimens

In the case of tests where the crack width is not recorded, it must be estimated from measurement of the actual deflection. Although the relationship is not direct, and depends on the depth of cracking, a good estimate can be obtained as follows.

If the deflection f_0 at the end of the elastic range is known (see paragraph 7.2), the crack width (w) can be estimated using the following equation:

$$w = 4/3 * 0.9 * (f - f_0)$$

where f is the actual deflection as measured.

This expression is derived from the assumption of a perfect hinge mechanism at the crack, modified by a correction factor taking account of the fact that the crack does not go right through the section. It is therefore not valid in the initial phase of crack propagation. However, this phase is relatively short and the depth of the crack quickly stabilizes between 80% and 90% of the depth of the section.

Remark: This approach must be used only as a last resort, given the diversity of responses from one concrete to another.

7.4. Filtering of data, centre-point bending, notched specimens

The purpose of data filtering is to reduce the noise of test data in order to facilitate back analysis. Naturally, the better the quality of the tests, the easier the filtering operation is. Whenever a test result has sudden jumps in either force or displacement (deflection or crack width), obviously resulting from control problems during the test, no filtering should be carried out in an attempt to give a physical meaning to the recorded behaviour.

110 - Recommandations provisoires

problèmes d'asservissement lors de l'essai, aucun filtrage ne doit être mis en œuvre pour tenter de donner un sens physique à un tel comportement. Par suite, un tel résultat d'essais doit tout simplement être rejeté pour une analyse ultérieure. Une description suffisante du comportement peut être obtenue avec échantillonnage des résultats sur un pas d'ouverture de fissure de 20 micromètres. Une méthode simple consiste alors à effectuer la moyenne des efforts enregistrés sur un intervalle de 40 micromètres et à affecter cette valeur au point central de l'intervalle. Compte tenu de la fréquence d'échantillonnage retenue (5 Hz) et de la vitesse de pilotage adoptée, cette technique de moyenne mobile est facile à mettre en œuvre et revient à moyenniser un nombre de données assez important sur chaque intervalle.

Remarque : au niveau de l'origine des courbes, le premier point est le point expérimental qui définit la fin du domaine élastique. Il ne fait l'objet d'aucune moyenne. Dès le deuxième point, la moyenne mobile peut être mise en œuvre en agrandissant progressivement l'intervalle sur lequel est calculée la moyenne.

8. Extraction de la loi de traction par méthode inverse

Cette partie a pour objectif de donner le principe de la méthode inverse qui permet d'obtenir une relation contrainte de traction en fonction de l'ouverture de la fissure à partir des résultats expérimentaux moment résistant en fonction de l'ouverture de la fissure, obtenus dans le cadre des essais de flexion 3 points sur prismes entaillés. La méthode de calcul présentée doit être appliquée sur les données filtrées afin d'obtenir une convergence numérique stable.

8.1. Equilibre mécanique de la section fissurée

La figure suivante illustre une section fissurée d'un prisme en flexion. Deux parties sont distinguées, celle non fissurée où la distribution des contraintes correspond à un comportement élastique linéaire, et celle fissurée où la distribution des contraintes dépend directement de l'efficacité des fibres.

meaning to the recorded behaviour. Consequently such test results must simply be rejected for subsequent analysis.

An adequate description of behaviour can be obtained by sampling results at crack-width steps of 20 micrometres. A simple method of achieving this is to average the forces recorded over a 40 micrometre interval and attribute that mean value to the centre of the interval. Given the frequency of sampling (5 Hz) and loading rate adopted, this moving-average technique is easy to use, and involves averaging quite a large amount of data for each interval.

Remark: At the origin of the curves, the first point is the test point defining the end of the elastic range. It is not averaged. The moving average can be used for the second point and beyond, gradually increasing the averaging interval.

8. Extraction of the tensile-strength law using back analysis

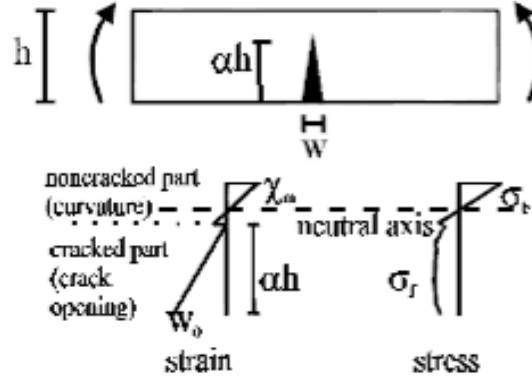
The purpose of this section is to outline the principle of back analysis which will produce a tensile stress/crack width relationship from resistance moment/crack width test results obtained with centre-point flexural tests on notched prisms. The calculation method presented must be applied to filtered data in order to obtain stable numerical convergence.

8.1. Mechanical equilibrium of the cracked section

The figure below shows a cracked section of a bent prism. Two different parts are distinguished: the uncracked part where the stress distribution corresponds to linear elastic behaviour, and the cracked part where stress distribution depends directly on the effectiveness of the fibres. It is the latter distribution which is of interest here, and which can be determined by back analysis

C'est cette dernière distribution que l'on recherche et qui résulte de l'exploitation par la méthode inverse [1.11], [1.12], [1.13].

which can be determined by back analysis [1.11], [1.12], [1.13].



L'équilibre mécanique de la section conduit aux équations suivantes, en notant b la contribution de la partie non fissurée et f , celle de la partie fissurée :

The mechanical equilibrium of the section results in the following equations, where b is the contribution of the uncracked part and f the contribution of the cracked part:

$$N_b = \frac{E \cdot \chi_m \cdot b \cdot h^2}{2} \left[(1 - \alpha_n)^2 - (\alpha - \alpha_n)^2 \right]$$

$$N_f = \frac{\alpha \cdot h \cdot b}{w_0} \int_0^{w_0} \sigma_f \cdot dw$$

$$M_f = \alpha h N_f - \frac{(\alpha h)^2 \cdot b}{w_0} \int_0^{w_0} \sigma_f \cdot w \cdot dw$$

$$M_b = \frac{E \cdot \chi_m \cdot b \cdot h^3}{3} \left[(1 - \alpha_n)^3 - (\alpha - \alpha_n)^3 \right] + h \cdot \alpha_n \cdot N_b$$

soit : moment résistant : $M = Mb + Mf$
effort normal : $N = Nb + Nf = 0$

i.e. resistance moment: $M = Mb + Mf$
normal force: $N = Nb + Nf = 0$

avec :
 α la hauteur relative de la fissure (voir figure)
 α_n la hauteur relative de l'axe neutre donnée par : $\sigma_t = E \cdot \chi_m \cdot h \cdot (\alpha - \alpha_n)$
 χ_m la courbure de la partie non fissurée
 σ_t la résistance en traction de la matrice
 E le module élastique
 b, h la largeur et la hauteur de la section

with:
 α relative depth of the crack (see figure)
 α_n relative height of the neutral fibre, given by: $\sigma_t = E \cdot \chi_m \cdot h \cdot (\alpha - \alpha_n)$
 χ_m curvature of the uncracked part
 σ_t tensile strength of the matrix
 E modulus of elasticity
 b, h breadth and height of the section

Pour relier l'ouverture de la fissure à la courbure de la partie non fissurée, une relation cinématique est utilisée de la forme suivante :

To link crack width to the curvature of the uncracked part, a kinematic relationship of the following type is used:

112 - Recommandations provisoires

$$w_0 = [\chi_m + 2 \cdot \chi_e] \frac{2 \cdot (\alpha h)^2}{3}$$

avec : χ_e la courbure élastique équivalente, donnée par : $\chi_e = M/EI$ et I l'inertie de la section rectangulaire

8.2. Processus itératif

Dans la mesure où la relation contrainte de traction en fonction de l'ouverture de la fissure n'a pas une forme simple, nous recherchons des couples de points (w_i, σ_{fi}), qui la définissent de façon discrète. Considérant alors que la discrétisation de l'abscisse qui correspond aux ouvertures de fissure est suffisamment fine, nous pouvons exprimer l'intégrale des contraintes par une approximation trapèze, soit par exemple :

$$\int_0^{w_{i+1}} \sigma_f \cdot dw = \int_0^{w_i} \sigma_f \cdot dw + \left(\frac{\sigma_{fi} + \sigma_{fi+1}}{2} \right) (w_{i+1} - w_i)$$

Par suite, les expressions précédentes de l'effort normal et du moment de la partie fissurée peuvent être exprimées de façon incrémentales :

$$N_{fi+1} = N_{fi} \cdot \frac{\alpha_{i+1}}{\alpha_i} \cdot \frac{w_i}{w_{i+1}} + \alpha_{i+1} \cdot b \cdot h \cdot \left(\frac{\sigma_{fi} + \sigma_{fi+1}}{2} \right) \left(1 - \frac{w_i}{w_{i+1}} \right)$$

$$M_{fi+1} = M_{fi} \left(\frac{\alpha_{i+1}}{\alpha_i} \cdot \frac{w_i}{w_{i+1}} \right)^2 + \alpha_{i+1} \cdot h \cdot N_{fi+1} \left(1 - \frac{w_i}{w_{i+1}} \right) - \frac{(\alpha_{i+1} \cdot h)^2 \cdot b}{2} \left(1 - \frac{w_i}{w_{i+1}} \right)^2 \cdot \sigma_{fi+1}$$

Ainsi, considérant que la relation contrainte ouverture de fissure est connue jusqu'à l'itération i , nous obtenons les deux inconnues contrainte et hauteur relative de la fissure à l'itération $i+1$ en mettant en œuvre les équations du modèle précédent, de façon à satisfaire la nullité de l'effort normal et un moment résistant de la section égale au moment expérimental.

8.3. Initialisation du procédé et stabilisation de la convergence

Afin de démarrer le processus incrémental, il

$$w_0 = [\chi_m + 2 \cdot \chi_e] \frac{2 \cdot (\alpha h)^2}{3}$$

where: χ_e is the equivalent elastic curvature, given by $\chi_e = M/EI$ and I is the inertia of the rectangular section.

8.2. Iterative process

Since the tensile stress/crack width relationship is complex, couples of points (w_i, σ_{fi}) defining it discretely are sought. Considering that the discretization of the horizontal scale (crack width) is sufficiently fine, the integral of the stresses can be expressed by a trapezoidal approximation such as:

Subsequently, the previous expressions of the normal force and moment of the cracked part can be expressed incrementally:

Thus, considering that the stress/crack width relationship is known to iteration i , the two unknowns—stress and relative depth of the crack at iteration $i+1$ —can be calculated with the equations of the previous model so as to obtain zero normal force and a resistance moment of the section equal to the test moment.

8.3. Initialization of the process and stabilization of convergence

To start the incremental process, take as



suffit de prendre pour valeurs initiales le point défini comme moment de fissuration (fin du domaine élastique), avec une ouverture de fissure nulle :

$$M_b^0 = M_{\text{ext}} = \frac{-bh^2 \cdot \sigma_f^0}{6}$$

avec $M_f^0 = 0$; $N_b^0 = 0$; $N_f^0 = 0$

Dans la mesure où la description des résultats expérimentaux est discrète, la méthode inverse mettant en œuvre une sorte de dérivée de la courbe des moments, une oscillation de la relation contrainte en fonction de l'ouverture de la fissure est fréquente. Afin de stabiliser ce phénomène, nous avons pu vérifier qu'il suffit de corriger l'itération i après avoir calculé l'itération $i+1$.

En pratique, il suffit de repositionner la contrainte de l'itération i en effectuant une moyenne mobile du type suivant :

$$\sigma_i = (2 \cdot \sigma_i + \sigma_{i+1})/3$$

Dans la mesure où la contrainte ne varie pas brusquement, et c'est le cas en pratique, cette correction n'affecte pas la réponse de la méthode et conduit à des résultats beaucoup plus réalistes. Notons que cette opération de stabilisation doit être effectuée à la fin de chaque itération afin d'être prise en compte lors du calcul des itérations suivantes.

8.4. Correction de l'effet d'échelle

Il a été décidé de retenir dans certains cas l'essai de flexion 3 points sur prisme entaillé. En fait, l'objectif de l'entaille a simplement pour but de localiser la fissure dans une section précise et en aucun cas de se placer dans les hypothèses de la mécanique de la rupture qui considèrent un rayon de courbure nul en fond d'entaille. Par suite, la fissuration qui correspond à la perte de linéarité de la courbe des moments est affectée d'un effet d'échelle, tout comme dans le cas des essais de flexion sur prismes non entaillés.

Il est donc nécessaire de corriger cet effet afin d'obtenir une valeur réaliste de la contrainte de fissuration. L'approche retenue est similaire à

starting values the point defined as the cracking point (end of the elastic range), with a crack width of zero:

$$M_b^0 = M_{\text{ext}} = \frac{-bh^2 \cdot \sigma_f^0}{6}$$

with $M_f^0 = 0$; $N_b^0 = 0$; $N_f^0 = 0$

Since the description of the test results is discrete, the back-analysis method using a sort of derivative of the moment curve, oscillation of the stress/crack width relationship often occurs. It has been shown that it can be stabilized by correcting iteration i after calculating iteration $i+1$.

In practice, it is sufficient to reposition the stress of iteration i by determining a moving average of the following type:

$$\sigma_i = (2 \cdot \sigma_i + \sigma_{i+1})/3$$

If the stress does not vary suddenly—which is the case in practice—this correction does not affect the response of the method and leads to much more realistic results. It should be observed that this stabilization operation must be carried out at the end of each iteration in order to be taken into account in the calculation of the following iterations.

8.4. Correction of scale effect

In some cases it was decided to adopt the centre-point flexural test with notched prisms. The purpose of the notch is simply to initiate the crack in a specific section, and has nothing to do with the assumptions of fracture mechanics considering a zero radius of curvature at the bottom of the notch. Accordingly, the cracking which corresponds to loss of linearity of the moment curve is affected by scale effect, as in the case of flexural tests on un-notched prisms.

It is therefore necessary to correct the scale effect to obtain a realistic value for the cracking stress. The approach adopted is

114 - Recommandations provisoires

fissuration. L'approche retenue est similaire à celle exposée au paragraphe 7.1 :

$$R_t = R_{ft} * \frac{2.0 * \left(\frac{h}{h_0}\right)^{0.7}}{1 + 2.0 * \left(\frac{h}{h_0}\right)^{0.7}} \quad \text{avec } h_0 = 100 \text{ mm}$$

cracking stress. The approach adopted is similar to that outlined in paragraph 7.1:

Pour appliquer une telle formule, il faut adopter pour h, la hauteur réduite de la section, c'est à dire la hauteur résiduelle après entaille, soit 0,9a. En soi, cette valeur a un caractère purement numérique et en aucun cas elle ne peut être considérée comme représentative de la vraie résistance en traction du matériau.

To apply a formula such as this, h must be taken as the reduced depth of the section, i.e. the residual thickness after notching, i.e. 0.9a. In itself this value is of a purely numerical nature and under no circumstances can be considered to be representative of the actual tensile strength of the concrete.

Par contre, l'effet de l'entaille disparaît rapidement lorsque la fissure se propage et nous avons pu vérifier que dans la cadre de la mise en œuvre de la méthode inverse, il est préférable de considérer le prisme comme non entaillé, c'est à dire ayant une hauteur non réduite. Sans qu'il soit possible de justifier rationnellement cette observation, nous pouvons simplement constater que dans tous les cas, une telle position tend à réduire les contraintes dans la fissure et donc nous place du côté de la sécurité.

On the other hand, the effect of the notch quickly disappears as the crack propagates, and it has been demonstrated that when the back-analysis method is used, it is preferable to consider the prism as un-notched, i.e. not with the reduced depth. Although it is not possible to rationally substantiate this observation, it can simply be observed that in all cases this approach tends to reduce the stresses in the crack and therefore puts things on the safe side.

SINTEF Building and Infrastructure is the third largest building research institute in Europe. Our objective is to promote environmentally friendly, cost-effective products and solutions within the built environment. SINTEF Building and Infrastructure is Norway's leading provider of research-based knowledge to the construction sector. Through our activity in research and development, we have established a unique platform for disseminating knowledge throughout a large part of the construction industry.

COIN – Concrete Innovation Center is a Center for Research based Innovation (CRI) initiated by the Research Council of Norway. The vision of COIN is creation of more attractive concrete buildings and constructions. The primary goal is to fulfill this vision by bringing the development a major leap forward by long-term research in close alliances with the industry regarding advanced materials, efficient construction techniques and new design concepts combined with more environmentally friendly material production.

